Upregulation of Human Endogenous Retrovirus-K Is Linked to Immunity and Inflammation in Pulmonary Arterial Hypertension

Editorial, see p 1936

Toshie Saito, MD
et al

BACKGROUND: Immune dysregulation has been linked to occlusive vascular remodeling in pulmonary arterial hypertension (PAH) that is hereditary, idiopathic, or associated with other conditions. Circulating autoantibodies, lung perivascular lymphoid tissue, and elevated cytokines have been related to PAH pathogenesis but without a clear understanding of how these abnormalities are initiated, perpetuated, and connected in the progression of disease. We therefore set out to identify specific target antigens in PAH lung immune complexes as a starting point toward resolving these issues to better inform future application of immunomodulatory therapies.

METHODS: Lung immune complexes were isolated and PAH target antigens were identified by liquid chromatography tandem mass spectrometry, confirmed by enzyme-linked immunosorbent assay, and localized by confocal microscopy. One PAH antigen linked to immunity and inflammation was pursued and a link to PAH pathophysiology was investigated by next-generation sequencing, functional studies in cultured monocytes and endothelial cells, and hemodynamic and lung studies in a rat.

RESULTS: SAM domain and HD domain-containing protein 1 (SAMHD1), an innate immune factor that suppresses HIV replication, was identified and confirmed as highly expressed in immune complexes from 16 hereditary and idiopathic PAH versus 12 control lungs. Elevated SAMHD1 was localized to endothelial cells, perivascular dendritic cells, and macrophages, and SAMHD1 antibodies were prevalent in tertiary lymphoid tissue. An unbiased screen using metagenomic sequencing related SAMHD1 to increased expression of human endogenous retrovirus K (HERV-K) in PAH versus control lungs (n=4). HERV-K envelope and deoxyuridine triphosphate nucleotidohydrolase mRNAs were elevated in PAH versus control lungs (n=10), and proteins were localized to macrophages. HERV-K deoxyuridine triphosphate nucleotidohydrolase induced SAMHD1 and proinflammatory cytokines (eg, interleukin 6, interleukin 1β, and tumor necrosis factor α) in circulating monocytes, pulmonary arterial endothelial cells, and also activated B cells. Vulnerability of pulmonary arterial endothelial cells (PAEC) to apoptosis was increased by HERV-K deoxyuridine triphosphate nucleotidohydrolase in an interleukin 6-independent manner. Furthermore, 3 weekly injections of HERV-K deoxyuridine triphosphate nucleotidohydrolase induced hemodynamic and vascular changes of pulmonary hypertension in rats (n=8) and elevated interleukin 6.

CONCLUSIONS: Our study reveals that upregulation of the endogenous retrovirus HERV-K could both initiate and sustain activation of the immune system and cause vascular changes associated with PAH.

The full author list is available on page 1933.

Correspondence to: Marlene Rabinovitch, MD, Stanford University School of Medicine, CSSR 1215A, 269 Campus Drive, Stanford, CA 94305. E-mail marlener@stanford.edu

Sources of Funding, see page 1933

Key Words: deoxyuridine triphosphate nucleotidohydrolase (dUTPase) ■ human endogenous retrovirus K (HERV-K) ■ pulmonary arterial hypertension (PAH) ■ SAM domain and HD domain-containing protein 1 (SAMHD1) ■ tertiary lymphoid tissue

Clinical Perspective

What Is New?

- SAM domain and HD domain-containing protein 1 (SAMHD1) is an innate immune factor that suppresses HIV replication. We identified SAMHD1 immune complexes in lungs from patients with pulmonary arterial hypertension (PAH).
- Elevated SAMHD1 led to the discovery that human endogenous retrovirus (HERV-K) gene products, HERV-K envelope and deoxyuridine triphosphate nucleotidohydrolase (dUTPase), were elevated in lungs with PAH.
- Heightened expression of HERV-K dUTPase was observed in PAH circulating monocytes and induced pluripotent stem cells.
- Treatment with HERV-K dUTPase induced SAMHD1 and cytokines, including interleukin 6, in circulating monocytes and pulmonary arterial endothelial cells and promoted apoptosis in pulmonary arterial endothelial cells (PAECs).
- Rats treated with HERV-K dUTPase developed pulmonary hypertension.

What Are the Clinical Implications?

- Current treatments for PAH improve survival but are not disease modifying because they do not address the pathological mechanisms of inflammation and immune dysregulation.
- We show that perivascular immune complexes containing the antiviral protein SAMHD1 result from elevation in products of the endogenous retrovirus HERV-K that are expressed in PAH perivascular macrophages and circulating monocytes.
- The HERV-K dUTPase activates B cells, elevates cytokines in monocytes and pulmonary arterial endothelial cells, and increases pulmonary artery vulnerability to apoptosis, thus contributing to sustained inflammation, immune dysregulation, and progressive obliterative vascular remodeling.
- Mechanisms that normalize HERV-K expression could prevent and reverse PAH.

Pulmonary arterial hypertension (PAH) is a progressive disorder that may be idiopathic, hereditary, or associated with other conditions that include immune/inflammatory diseases such as scleroderma or HIV infection. In all cases, PAH is characterized by endothelial cell (EC) dysfunction, loss of distal pulmonary arteries (PAs), and obliterative changes in more proximal PAs in association with exuberant expansion of cells that progressively occlude the vessel lumen. These features contribute to an elevation in right ventricular systolic pressure, which, despite vasodilator therapy, can lead to right heart failure and the need for a lung transplant. Inflammatory and autoimmune processes are inextricably linked to vascular remodeling in PAH.[1] Circulating autoantibodies,[2] lung perivascular tertiary lymphoid tissue,[3] and elevated cytokines, including interleukin (IL) 6, tumor necrosis factor α, and IL1β[4], have been reported in patients with PAH.

The link between immunity and clinical PAH is also evident in experimental animal studies. For example, the athymic rat develops severe pulmonary hypertension attributed to a lack of regulatory T cells.[5] Production of pathological antibodies by bronchus-associated lymphoid tissue is observed in monocrotaline-induced pulmonary hypertension in rats.[6] However, specific target antigens in lung immune complexes have not been reported in either PAH or experimental pulmonary hypertension. This finding could provide mechanistic insight into factors that initiate and perpetuate immune dysregulation and their role in the pathophysiology of PAH.

METHODS

Expanded Materials and Methods are provided in the Online-Only Data Supplement.

Human Samples From Patients With PAH and Controls

All human samples used in this study were deidentified but had been obtained by written informed consent under protocols approved by the Administrative Panel on Human Subjects in Medical Research at the various sites described in the online-only Data Supplement. The demographic and other characteristics of patients with PAH and healthy controls used in the various studies are provided in Tables I and II in the online-only Data Supplement.

Lung Tissue

Lung tissues from patients with hereditary and idiopathic PAH and control subjects (unused donor lungs) were processed and stored as described previously.[7]

Cell Isolation and Culture

Pulmonary arterial endothelial cells (PAECs)[8] and PA smooth muscle cells (PASMCs)[9] from patients with PAH and donor control were harvested as described previously. In some experiments, we used commercially available PAECs. PAECs were cultured in EC media supplemented with 5% fetal bovine serum, EC growth supplement, and penicillin/streptomycin and used at passage 3 to 6. PASMCs were cultured in SMC media supplemented with 5% fetal bovine serum, SMC growth supplement, and gentamicin/amphotericin-B and used at passage 4 to 10. Induced pluripotent stem cells derived from fibroblasts and differentiated ECs were generated by previously published protocols.[8,10]

Peripheral Blood Mononuclear Cells

Peripheral blood mononuclear cells (PBMCs) were separated by Ficoll-Paque after centrifugation of whole blood at 400 g for 30 minutes. PBMCs ($1x10^7$) were used for further preparation of enriched monocytes. Cells that attached to wells after 2 hours represented an enriched monocyte preparation.

For detection of human endogenous retrovirus K deoxyuridine triphosphate nucleotidohydrolase (HERV-K dUTPase) in monocytes by quantitative polymerase chain reaction (PCR), we used the Pan Monocyte Isolation kit according to the manufacturer's protocol. PBMCs were cultured with RPMI-1640 and supplemented with 10% fetal bovine serum and penicillin/streptomycin.

HERV-K dUTPase Protein Purification

Recombinant HERV-K dUTPase protein was provided by Dr Ariza. The HERV-K gene encoding the dUTPase was cloned into the pTrcHis Topo TA expression vector, and the sequence was verified by DNA sequencing analysis as previously described.[11] The purity of the protein was assessed by SDS-PAGE and capillary-liquid chromatography nanospray tandem mass spectrometry performed at the Ohio State University Mass Spectrometry and Proteomics Facility.[11] High-purity dUTPase preparations,[11] free of contaminating DNA, RNA, lipopolysaccharide, and peptidoglycan, were used.

Treatment of Cells With HERV-K dUTPase Recombinant Protein or Lipopolysaccharide

PAECs (1x10^6), PBMCs (1x10^6), or enriched monocytes (isolated from 1x10^7 PBMCs as described earlier) were used. Cells were incubated with 0.1, 1.0, or 10 µg/mL of recombinant HERV-K dUTPase for 24 hours. Culture supernatants were collected for cytokine measurement by enzyme-linked immunosorbent assay (ELISA), and cell lysates were used for western immunoblotting. PBMCs were analyzed by single mass cytometry. PAECs were also assessed for apoptosis judged by heightened caspase activity during serum withdrawal[8] for 16 hours, when HERV-K dUTPase was added. PASMCs were assessed for proliferation (3-[4,5-Dimethylthiazol-2-Yl]-2,5-Diphenyltetrazolium Bromide [MTT] cell proliferation assay) in response to HERV-K dUTPase for 48 hours. In some experiments, IL6 neutralizing antibody versus isotype control was used to assess whether PAEC apoptosis induced by HERV-K dUTPase was IL6-dependent. In some experiments, monocytes and PAECs were treated with 1 µg/mL lipopolysaccharide for 6 hours, and cell lysates were used for quantitative PCR to assess HERV-K dUTPase mRNA.

Immunohistochemistry

Formaldehyde-fixed, paraffin-embedded tissue sections were deparrafinized and permeabilized with 0.2% Triton. Antigen retrieval was done with either citrate buffer pH 6.0 or 1 mM EDTA pH 8.0 depending on the primary antibodies. Sections were immersed in 0.3% hydrogen peroxide, blocked with 5% goat serum, and stained with primary antibodies. The following primary antibodies were used: SAMHD1 (1:500), CD3 (1:50), CD19 (1:100), plasma cell (1:100), follicular dendritic cell (1:50), and IL6 (1:1000). After incubation with secondary antibodies and amplification with streptavidin-biotin, sections were stained with 3,3-diaminobenzidine and counterstained with hematoxylin.

Immunofluorescent Staining

Tissue sections were processed as described earlier using primary antibodies for SAMHD1 (1:500), von Willebrand factor (1:1000), CD11c (1:100), CD68 (1:100), CD3 (1:50), HERV-K env (1:1000), HERV-K dUTPase (1:2000, provided by Dr. Ariza), and α-Actin (1:400), followed by fluorescent-conjugated secondary antibodies, Alexa Fluor 488 anti-mouse (1:800), or Alexa Fluor 594 anti-rabbit antibodies (1:800). Nuclei were stained with DAPI. Images were acquired using a FlouView 1000 or a Leica TCS SP8 confocal microscope.

In Situ SAMHD1 Antibody Production

To localize SAMHD1 antibody-producing cells, frozen lung tissues were fixed with acetone blocked with 5% normal goat serum and incubated with GST-tagged SAMHD1 recombinant protein in PBS (20 µg/mL) overnight at 4˚C. Sections were washed with PBS and incubated with FITC-conjugated anti-GST antibody (1:800) for 1 hour at room temperature. Nuclei were stained with DAPI. Images were acquired using a FlouView 1000 confocal microscope.

Immune Complex Immunoprecipitation and Mass Spectrometry to Identify Target Antigens

Immune complexes were captured using a Direct IP kit according to the manufacturer's protocol. The samples were then prepared using filter-aided sample preparation.[12] After a buffer exchange, digestion using trypsin was performed on the membrane filter overnight at 37˚C, where peptides were spun out, collected, and further cleaned on C18 reverse phase material and analyzed by liquid chromatography and mass spectrometry. The raw data were converted to .mgf format and searched by Byonic (Protein Metrics) using typical search conditions, and a 1% false discovery rate was determined using the standard reverse decoy strategy. Byonic output files were further analyzed using custom scripts developed in Matlab to aid in data visualization. We excluded proteins where we did not observe at least 3 peptides in at least 1 sample. Common contaminants were also excluded. For all other proteins, control and PAH patient data were assessed using significance analysis of microarrays to determine q values and a false discovery rate cutoff of 5%.

Quantification of SAMHD1-Specific Immune Complexes

Lung tissue (100 mg) was lysed using a dounce homogenizer and 500 µl of lysis buffer (0.025 mol/L Tris-HCl pH 7.5, 0.15 mol/L NaCl, 1 mM EDTA, 0.5% NP40, 5% glycerol) with proteinase/phosphatase inhibitors. After centrifugation at 20 000 g for 20 minutes at 4˚C, total protein concentration of the supernatant was measured and diluted in PBS to 1 µg/µl total protein. ELISA plates were coated with 0.02 mg/mL SAMHD1 antibody in PBS overnight at 4˚C. The plates were blocked with 5% BSA in PBS for 1 hour. Lung lysate was applied and incubated for 2 hours. HRP-conjugated species-specific anti-human IgG added to the plates and incubated for 1 hour at room temperature. Tetramethylbenzidine substrate was added for 15 minutes, the reaction was stopped with 2 N sulfuric acid, and optical density values were determined at 450 nm.

Western Immunoblotting

Lung lysates (50 mg) were prepared by homogenization with 500 µl of modified RIPA buffer (50 mM Tris-HCl pH 7.4, 150 mM NaCl, 1 mM EDTA, 1% Triton X-100, 0.1% SDS, 1% sodium deoxycholate, 1 mM PMSF) containing protease and phosphatase inhibitors. After centrifugation at 20 000 g for 20 minutes at 4°C, the supernatant was collected. Protein concentration was determined by BCA. Equal amounts of protein were loaded on a precast NuPage 4% to 12% Bis-Tris gel and subjected to electrophoresis under reducing conditions and electrotransferred onto polyvinylidene difluoride membranes. After blocking with 5% milk in 0.5% Tween-PBS, membranes were incubated with primary antibodies against SAMHD1 (1:500), pSTAT3 (1:1000), STAT3 (1:1000), β-actin (1:10000), and α-tubulin (1:2000). Anti-mouse IgG secondary antibody (1:5000) was used. After incubation with HRP-conjugated secondary antibodies, signals were visualized with enhanced chemiluminescence or enhanced chemiluminescence prime.

Enzyme-Linked Immunosorbent Assay

Cytokine levels in human enriched monocytes, human PAECs, and rat lung lysates were measured using the Quantikine ELISA kit for human tumor necrosis factor α, IL1β, and IL6 and rat IL6 according to the manufacturer's protocol.

Quantitative PCR

Total RNA was extracted and purified from lung tissue or cells using spin column-based kits. Real-time PCR was performed according to the manufacturer's protocol. Quantitative PCR was performed with a 7900HT sequence-detection system or a CFX384 real-time system. Primers used were TaqMan gene expression assays, β-actin (Hs01060665_g1), HERV-K(II) env (PN4441114, custom probe, Applied Biosystems), Syber Green assays, HERV-K dUTPase (Forward, 5′-AAATGGGCAACCATTGTCGGGAAACGAGC-3′; Reverse, 5′-TAGTACATAAATCTACTGCTGCACTGC-3), and β-actin (Forward, 5′-CATGCCATCCTGCGTCTGGA-3′; Reverse, 5′-CCGTGGCCATCTCTTGCTCG).

Unbiased Pan-Viral Metagenomic Next-Generation Sequencing

Samples were sequenced on an Illumina MiSeq instrument using 300/200 base pair (bp) paired-end sequencing. Approximately 18.3 million sequencing reads were analyzed using a modified version of SURPI (Sequence-Based Ultra-Rapid Pathogen Identification),[13] a computational pipeline for the detection of microbes, including viruses, from next-generation sequencing data. Viral reads were identified as HERVs using a stringent edit distance requirement of 0 (no mismatches) across 75 bp of sequence. HERV reads were also taxonomically classified to the appropriate rank (family, genus, species, or subspecies/strain) by use of an in-house-developed classification algorithm using the SNAP nucleotide aligner (v0.15).[13] Heat maps were generated using matrix2png.[14]

Single Cell Mass Cytometry

PBMCs were stained with metal-conjugated antibodies and analyzed with a mass cytometer. $1x10^6$ cells were used for each sample. Concatenated data were normalized using NormalizerR2013b and debarcoded using the Matlab DebarcoderR2013b. Gating was performed in http://nolan-lab.cytobank.org.[15] The data were transformed to arcsinh values by taking the inverse hyperbolic sine of the raw data. The arcsinh ratio is the difference between the median arcsinh values of the 2 samples. Data from patients with PAH and controls are shown as arcsinh ratio normalized for assay control. Data for HERV-K dUTPase reflect treated over untreated (control) PBMCs (Stanford Blood Bank). Information about metal-conjugated antibodies is provided in the online-only Data Supplement.

Rat Model for the Induction of Pulmonary Hypertension by HERV-K dUTPase

The Animal Care Committee at Stanford University approved all experimental protocols used in this study after the published guidelines of the National Institutes of Health and the American Physiological Society. Adult male Sprague-Dawley rats (7 weeks, 180–200 g) were randomly assigned to a control or treatment group. Rats were either untreated or given a single subcutaneous dose of SU5416 (20 mg/kg body weight)[5] 1 day before the first of 3 weekly intravenous injections of HERV-K dUTPase (0.2 mg/kg body weight) in saline. Rats in the control group were treated with saline vehicle. Twenty-one days after the first HERV-K dUTPase injection, cardiac function, right ventricular systolic pressure, and right ventricular hypertrophy were assessed as previously described.[7] Isoflurane anesthesia (1.5%, 1 L/min oxygen) was used during these procedures. Lung tissues were assessed by histology and ELISA. For histology, staining methods are described earlier. Quantification of muscularization and arterial number relative to alveoli was conducted in a blinded manner, and details are provided in the online-only Data Supplement. Images were acquired using a Leica DMLB microscope (Leica). For the measurement of IL6 by ELISA, 20 µg of lung tissue were homogenized. After centrifugation, the total protein concentration of the supernatant was measured and prepared in PBS at a concentration of 0.5 µg/µL.

Statistical Analysis

Data were analyzed using Prism 6.0 (GraphPad Software). Statistical significance was determined by 1-way ANOVA followed by Dunnett's or Tukey's test of multiple comparisons when >2 groups were being compared. When only 2 groups were compared, we used Student's *t* test. For some experiments, as indicated in the figure legends, we applied the Welch or Mann-Whitney test depending on the data distribution (ie, when the distribution was not normal we used the Mann-Whitney, and when the variance was unequal by *F* test we used the Welch). A *P* value of <0.05 was considered significant. Data are shown as mean±SEM or median, with interquartile range depending on the test applied. For target identification of immune complexes by mass spectrometry, significance analysis of microarrays was applied with false discovery rate cutoff of 5%.[16] For signaling data by single mass cytometry, Bonferroni-adjusted *P* value ($P=7.14X10^{-3}$) was applied to signaling response with arcsinh ratio >|0.2|.[17]

A

Gene	PAH	PAH	PAH	CON	CON	CON
Tubulin beta chain	23	21	19	1	3	0
Clathrin heavy chain 1	8	11	8	0	0	0
Spectrin beta chain, brain 1	18	10	13	0	0	1
40S ribosomal protein S20	6	5	4	0	0	0
F-actin-capping protein subunit alpha-1	5	6	4	0	0	0
Myosin-Ib	21	17	8	0	0	0
Alpha-actinin-4	31	19	12	3	0	0
Actin-related protein 3	10	6	5	0	0	0
Myosin-11	276	166	85	32	8	0
Tropomodulin-3	23	13	8	0	0	0
Myosin-Id	31	8	21	0	0	0
Desmocollin-1	7	11	4	0	0	0
Actin-related protein 2	16	8	6	0	0	0
Eukaryotic translation initiation factor 2 subunit 3	4	11	7	1	0	0
rRNA 2"-O-methyltransferase fibrillarin	3	7	4	0	0	0
Actin, cytoplasmic 2	14	9	5	2	1	1
Myosin-Ic	56	34	12	2	3	2
Protein-glutamine gamma-glutamyltransferase 2	4	9	10	0	0	3
SAM domain and HD domain-containing protein 1	6	3	7	0	2	0
Actin-related protein 2/3 complex subunit 4	3	7	4	1	0	0
Myosin-9 OS	658	344	137	103	26	4
CD59 glycoprotein	3	5	2	0	0	0
40S ribosomal protein S13	7	9	9	1	6	4
40S ribosomal protein S3a	5	17	18	6	2	1
Gelsolin	47	25	10	12	2	1
ATP synthase subunit alpha, mitochondrial	14	12	16	12	8	9
Actin, cytoplasmic 1	143	153	80	115	38	31
Actin, aortic smooth muscle	17	3	10	0	3	1
Myosin light polypeptide 6	16	10	1	0	0	0

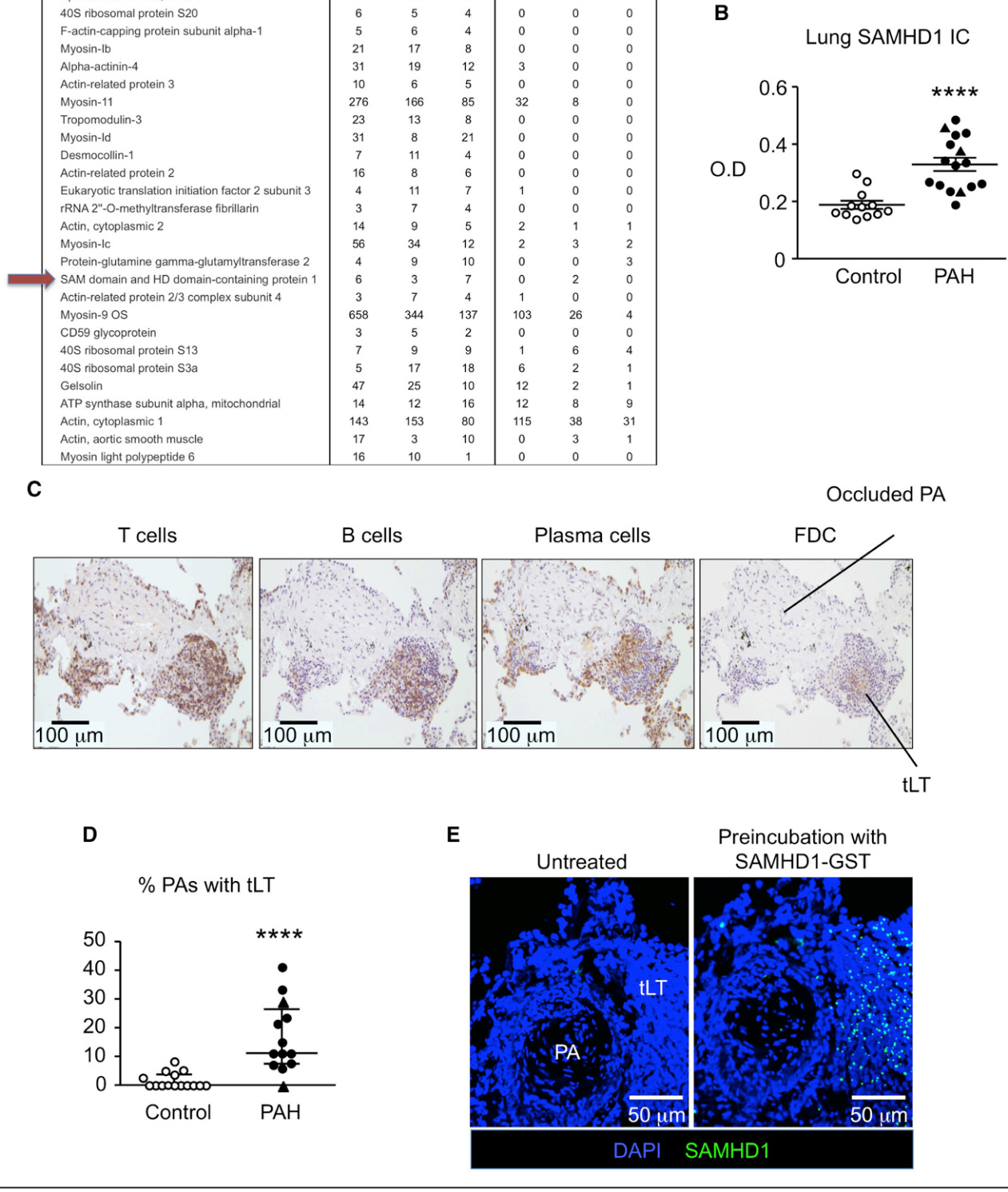

Figure 1. SAMHD1 a target antigen in immune complexes in PAH lungs.
A, C1q immunoprecipitation followed by liquid chromatography tandem mass spectrometry identified target antigens of immune complexes in PAH (n=3) and control (n=3) lungs. Targets are ranked by q value according to the significance analysis of microarrays, and all were within the false discovery rate (FDR) of 5%. **B,** SAMHD1 immune complexes measured by enzyme-linked immunosorbent assay (ELISA) in PAH (n=16) and control (n=12) lungs. ****P<0.0001 by Welch test. **C,** Representative sections from a PAH lung show tertiary lymphoid tissue (tLT), characterized by positive immunoreactivity to markers of T cells (CD3), (*Continued*)

Accession Numbers

Next-generation sequencing data with human sequences removed, using BLASTn to the human genome at a low-stringency cutoff of 10^{-5}, have been publicly deposited in the National Institutes of Health Sequence Read Archive (accession number SRP056561).

RESULTS

SAMHD1 Is a Target Antigen in Immune Complexes in PAH Lungs

We obtained lung tissues from unused donor lungs as controls and from patients with idiopathic or hereditary PAH (designated as PAH in the text) from the Pulmonary Hypertension Breakthrough Initiative Network. The characteristics of patients with PAH and controls are provided in Tables I and II in the online-only Data Supplement. To determine whether the target antigens of lung immune complexes differed in PAH versus control lungs, 3 PAH and 3 control lung samples were captured by complement 1q (C1q) immunoprecipitation, eluted, subjected to filter-aided sample preparation,[12] and analyzed by liquid chromatography tandem mass spectrometry. The top samples ranked based on q value and a false discovery rate <5%[16] are shown in Figure 1A. Of particular interest was SAMHD1, which was highly represented in PAH samples versus controls. SAMHD1 has been related to autoimmunity[18] and HIV infection,[19] conditions associated with PAH.

We therefore expanded our analysis to a larger cohort of 16 PAH and 12 control lungs and confirmed a significant increase in the level of SAMHD1 immune complexes in the PAH lungs (Figure 1B). We next investigated the source of the SAMHD1 antibodies in lungs with PAH. Tertiary lymphoid tissue, which is associated with chronic inflammation and autoimmune diseases,[20] is particularly prominent in lungs with PAH.[3] We confirmed these findings (Figure 1C and 1D) and investigated whether the tertiary lymph nodes are the source of SAMHD1 antibodies. After the addition of recombinant GST-tagged SAMHD1 protein to lung tissue sections and incubation of the tissue with an anti-GST-FITC-conjugated antibody, we observed SAMHD1 immunoreactive foci in the perivascular tertiary lymphoid tissue (Figure 1E), suggesting that these structures are the likely source of SAMHD1 antibody production.

Elevated SAMHD1 in Lung Cells With PAH and in Circulating Classical Dendritic Cells

In lungs with PAH, SAMHD1 immune complexes were associated with a heightened expression of SAMHD1 in lung lysates as assessed by western immunoblot (Figure 2A). The site of increased expression of SAMHD1 in lungs with PAH was localized to the perivascular region as well as the vessel wall, whereas in control lungs, SAMHD1-positive cells were scattered in the lung parenchyma and excluded from the arterial walls (Figure 2B). To determine the cellular localization of SAMHD1, we performed confocal microscopy analysis in tissue sections double-immunolabeled with antibodies to SAMHD1 and either von Willebrand factor to detect PAECs, CD68 as a marker of macrophages, CD11c for dendritic cells, and CD3 for T cells (Figure 2C). Almost all SAMHD1-positive cells in the perivascular/vascular region coexpressed markers for macrophages, dendritic cells, and ECs, but not for T cells. The heightened expression of SAMHD1 in PAH was also confirmed in circulating classical dendritic cells (Figure 2D, with details of gating in Figure IA in the online-only Data Supplement) assessed as part of a larger analysis applying single cell mass cytometry[15] to PBMCs.

HERV-K and Its Products HERV-K Envelope and dUTPase Are Increased in Idiopathic PAH

We next investigated whether SAMHD1 could be induced as an innate immune response[21] to an exogenous virus. In addition to HIV,[22] the Kaposi sarcoma virus (Human herpesvirus 8)[23] and hepatitis C virus[24] have been associated with PAH in some series but not others.[25] We therefore subjected flash-frozen lung tissue from 4 patients with PAH and 4 controls to a blinded unbiased metagenomic viral screen using the Illumina MiSeq next-generation sequencing platform and the SURPI computational pipeline to identify viral sequences.[13,26] Consistent with a previous series,[25] we did not detect

Figure 1 Continued. B cells (CD19), plasma cells (rough endoplasmic reticulum-associated protein p63), and follicular dendritic cells (FDC; 120 kDa FDC protein). **D,** Number of PAs with associated tertiary lymphoid tissue relative to total PAs was calculated as a percentage from lung tissue sections in each control (n=15) and each PAH patient (n=13). ****P<0.0001 by Mann-Whitney test. **E,** SAMHD1 immunoreactive foci in tertiary lymphoid tissue detected by applying recombinant GST-tagged SAMHD1 protein to lung tissue sections, followed by an anti-GST-FITC conjugated antibody. Negative controls were treated with PBS, followed by anti-GST-FITC conjugated antibody. Nuclei were stained by DAPI (blue). Ranges represent mean±SEM (**B**) and median with interquartile range (**D**). Closed symbols (PAH), open symbols (controls), and closed triangles (hereditary PAH [HPAH]). CON indicates control; DAPI, 4′,6-diamidino-2-phenylindole; FDC, follicular dendritic cell; FITC, fluorescein isothiocyanate; GST, glutathione S-transferase; PA, pulmonary artery; PAH, pulmonary arterial hypertension; PBS, phosphate-buffered saline; SAMHD1, SAM domain and HD domain-containing protein 1.

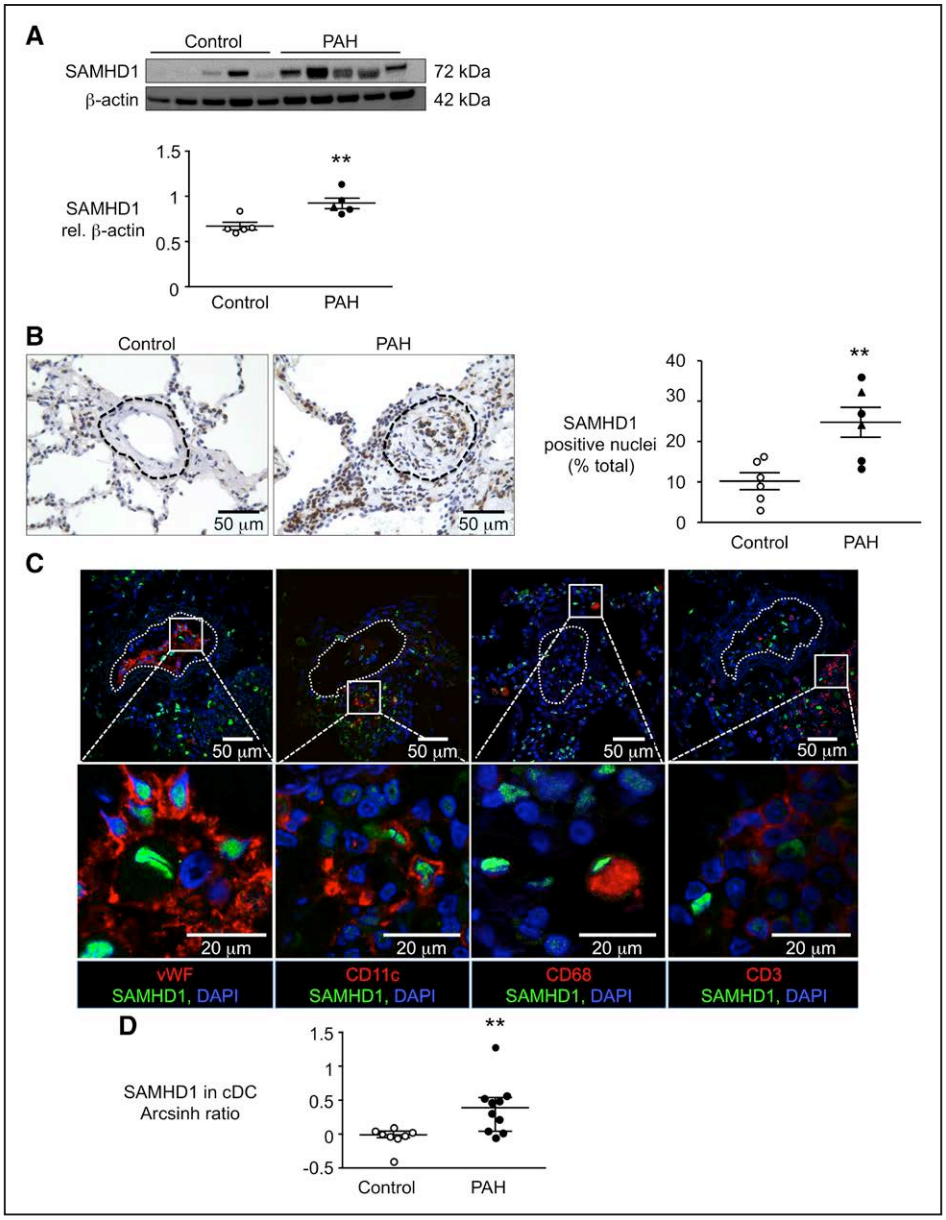

Figure 2. Elevated SAMHD1 in PAH lung cells and circulating classical dendritic cells (cDC).
A, Representative western immunoblot with densitometric quantitation of SAMHD1 in lung lysates assessed in PAH (n=5) versus control (n=5) lungs. ***P*<0.01 by Student's *t* test. **B,** Representative immunohistochemistry of SAMHD1 in pulmonary artery (PA) from a donor (control) lung and a PA of similar size and at a similar airway level from a lung of a patient with PAH (**left**), and percent nuclei that stained for SAMHD1 in all arteries in a lung section in PAH (n=6) versus control (n=6) lungs, calculated using the ImmunoRatio program (**right**). The dashed line indicates the vessel boundary including the adventitia, within which % SAMHD1-positive cells was calculated. ***P*<0.01 by Student's *t* test. **C,** Confocal microscopic images of sections immunolabeled with SAMHD1 (green) and four lineage markers (red), (left to right): von Willebrand factor (vWF) (endothelial cells), CD11c (dendritic cells), CD68 (macrophages), and CD3 (T cells). Nuclei were stained with DAPI (blue). Dashed line indicates vessel boundary. **D,** SAMHD1 assessed by single mass cytometry in circulating classical dendritic cells (cDCs) from patients with PAH (n=10) or controls (n=8). Data are shown as the calculated difference of inverse hyperbolic sine medians between control and samples with PAH (arcsinh ratio). ***P*<0.01 by Mann-Whitney test. Ranges represent mean±SEM (**A** and **B**) and median with interquartile range (**D**). Closed symbols (PAH), open symbols (controls), and closed triangles (hereditary PAH [HPAH]). DAPI, 4′,6-diamidino-2-phenylindole; PAH, pulmonary arterial hypertension; and SAMHD1, SAM domain and HD domain-containing protein 1.

viruses previously implicated in PAH in our lung samples, nor did we detect other known exogenous viruses. However, we observed a significant increase in the percentage of human endogenous retroviral sequences in lung samples with PAH relative to controls, in particular HERV-K[27] family members (Figure 3A).

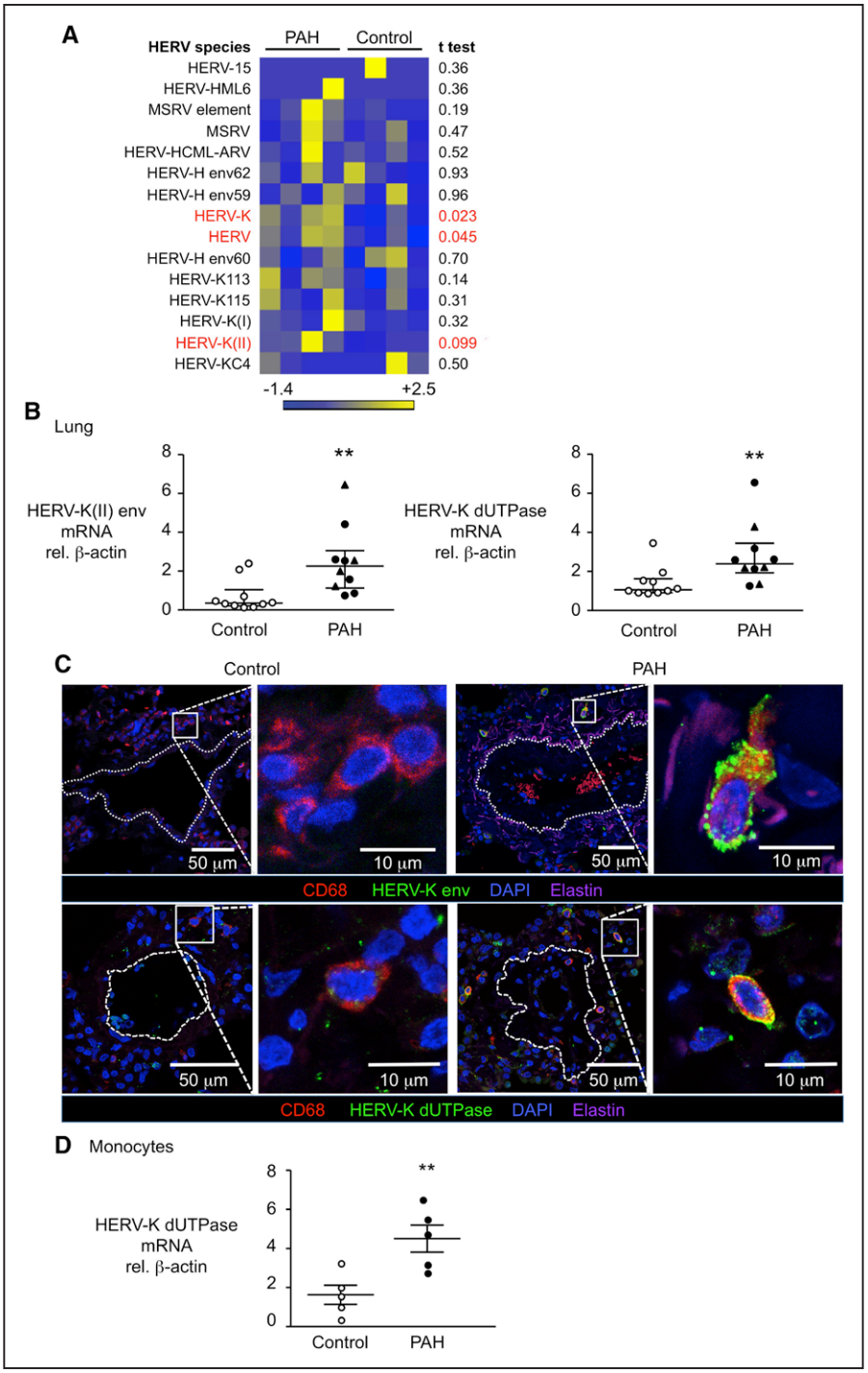

Figure 3. Elevated HERV-K and HERV-K dUTPase detected in lungs and circulating monocytes from PAH versus controls.

A, HERV species in lung tissue from patients with PAH (n=4) and controls (n=4) by metagenomic sequencing described in Methods. MSRV, multiple sclerosis-associated retrovirus. **B,** HERV-K(II) envelope and dUTPase mRNA by qPCR in lung extracts from patients with PAH (n=10) and controls (n=10). ***P*<0.01 by Mann-Whitney test. **C,** Confocal microscopy images of representative lung sections from a patient with PAH and a control show cells immunolabeled for HERV-K envelope protein or HERV-K dUTPase (green), macrophages (CD68+, red), and nuclei (DAPI, blue). Dashed line indicates vessel boundary. Elastin auto-fluorescence appears pink. **D,** HERV-K dUTPase mRNA in circulating monocytes from patients with PAH (n=5) versus controls (n=5). ***P*<0.01 by Student's *t* test. Ranges represent mean±SEM (**D**) and median with interquartile range (**B**). Closed symbols (PAH), open symbols (controls), and closed triangles (hereditary PAH [HPAH]). DAPI indicates 4′,6-diamidino-2-phenylindole; dUTPase, deoxyuridine triphosphate nucleotidohydrolase; HERV-K, human endogenous retrovirus K; PAH, pulmonary arterial hypertension; and qPCR, quantitative polymerase chain reaction.

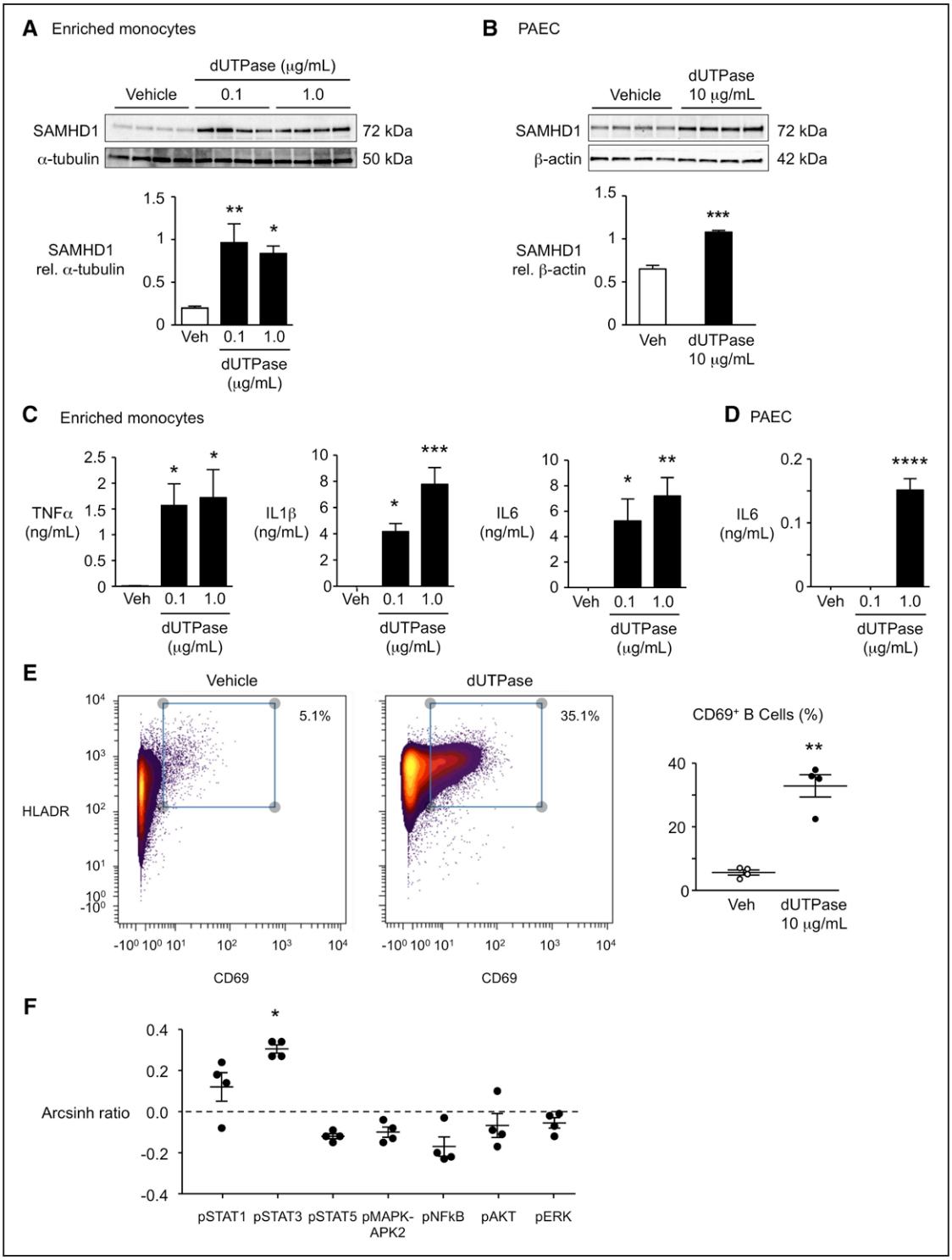

Figure 4. HERV-K dUTPase increases SAMHD1, cytokines in enriched monocytes, and pulmonary arterial endothelial cells (PAECs), as well as activates B cells.

Enriched monocytes from PBMCs (**A**) or PAECs (**B**) from healthy donors were treated with recombinant HERV-K dUTPase (0.1, 1, or 10 μg/mL) for 24 hours, and SAMHD1 was assessed by western immunoblot. TNFα, IL1β, and IL6 measured by enzyme-linked immunosorbent assay (ELISA) in medium of enriched monocytes (**C**) or PAECs (**D**) treated with 0.1 or 1 μg/mL HERV-K dUTPase. CD69⁺ B cells (**E**) and signaling molecules assessed by single mass cytometry (**F**) after HERV-K dUTPase (10 μg/mL for 24 hours). Signal induction was calculated as the difference of inverse hyperbolic sine medians between untreated (control) and HERV-K dUTPase-treated samples (arcshinh ratio). Ranges represent mean±SEM of 4 different experiments. **P*<0.05, ***P*<0.01, ****P*<0.001, *****P*<0.0001 by Student's *t* test (**B** and **E**) or 1-way ANOVA and post hoc Dunnett's test (**A**, **C**, and **D**). **F,** Bonferroni-adjusted *P* value ($P=7.14X10^{-3}$) is applied to response with arcsinh ratio >|0.2|). (*Continued*)

The HERV-K family comprises <1% of the HERV sequences found in the human genome and is transcriptionally active. Although in theory an infectious virus could be produced, mutations interrupting the virus open reading frame lead to degenerate sequences, which makes this highly unlikely. However, the expression of HERV-K-encoded proteins has been shown to induce viral restriction pathways in early embryonic cells.[28] Furthermore, the increased expression of HERV proteins, including the envelope protein and the dUTPase, has been linked to cancer,[29] multiple sclerosis,[30] systemic lupus erythematosus,[31] and rheumatoid arthritis.[32] Also, the psoriasis susceptibility 1 locus, identified as the strongest genetic determinant of psoriasis, harbors a HERV-K that encodes for a dUTPase.[33,34] We confirmed a significant induction in the HERV-K(II) envelope and HERV-K dUTPase mRNA in lungs with PAH versus controls (Figure 3B). Confocal microscopy demonstrated that an increase in HERV-K envelope and dUTPase proteins were primarily present in perivascular CD68+ macrophages, which are abundant in lungs with PAH (Figure 3C). We further confirmed that circulating monocytes from patients with PAH exhibit higher mRNA levels of HERV-K dUTPase relative to control cells (Figure 3D).

HERV-K dUTPase Increases SAMHD1 and Cytokines in Enriched Monocytes and PAECs and Activates B Cells

The HERV-K dUTPase induces the secretion of Th1 and Th17 cytokines involved in the formation of psoriatic plaques, independent of its enzymatic activity,[11] thus associating HERV-K to the pathology of psoriasis. Having confirmed the higher HERV-K dUTPase in PAH lung macrophages and circulating monocytes (Figure 3B through 3D), we determined whether recombinant HERV-K dUTPase could induce SAMHD1. Indeed, HERV-K dUTPase induces SAMHD1 in both enriched monocytes and PAECs (Figure 4A and 4B). Furthermore, in enriched monocytes, HERV-K dUTPase induces a profile of cytokines that are implicated in PAH, namely, tumor necrosis factor α, IL1β, and IL6[4], (Figure 4C). We also observed induction of IL6 by HERV-K dUTPase in PAECs (Figure 4D). Moreover, we found that HERV-K dUTPase can activate B cells, as determined by CD69 expression (Figure 4E, details of gating in Figure IB in the online-only Data Supplement), as well as STAT3 signaling (Figure 4F), consistent with a response related to the production of immunoglobulins.[35] Taken together, our observations related to the expansion of HERV-K and the sequelae of its dUTPase are consistent with chronic induction of inflammation and altered immunity observed in PAH.

HERV-K dUTPase Induces Apoptosis in PAECs

Because increased vulnerability to apoptosis is a feature of PAH PAECs,[8] we assessed the functional impact of HERV-K dUTPase on PAEC survival after serum withdrawal by the Caspase 3/7 assay. HERV-K dUTPase enhanced PAEC apoptosis after serum withdrawal (Figure 5A), as did coculture with HERV-K dUTPase-treated monocytes (Figure IIA in the online-only Data Supplement). To determine whether the enhanced PAEC apoptosis was related to the induction of IL6, we pretreated the cells with an IL6-neutralizing antibody versus an isotype control (Figure 5B). We verified the suppression of PBMC pSTAT3 in response to IL6 by the neutralizing antibody as a measure of its efficacy (Figure IIB in the online-only Data Supplement), but we could not detect a significant impact of blocking IL6 on HERV-K-mediated enhanced PAEC apoptosis (Figure 5B). HERV-K dUTPase had no effect on PASMC proliferation assessed by 3-(4,5-Dimethylthiazol-2-Yl)-2,5-Diphenyltetrazolium Bromide (MTT) assay at 48 hours (Figure IIC in the online-only Data Supplement).

HERV-K dUTPase Is Induced by Inflammatory Stimuli

Because circulating PAH monocytes have increased HERV-K dUTPase expression and are exposed to a high-cytokine milieu,[4] we determined whether inflammatory stimuli that can be genotoxic[36] could upregulate HERV-K dUTPase mRNA. Indeed, lipopolysaccharide treatment increased HERV-K dUTPase in monocytes (Figure 5C) but not in PAECs (Figure IID in the online-only Data Supplement). To determine whether the induction of HERV-K could be cell-specific, we also evaluated HERV-K dUTPase mRNA levels in induced pluripotent stem cells (iPSCs) because reprogramming of fibroblasts is known to induce an inflammatory response.[37] In fact, in a previous study, HERVs were transiently hyperactivated during reprogramming toward iPSCs and played an important role in this process.[38] However, once reprograming is complete and cells acquire full pluripotency, HERV activity decreases.[38] iPSCs from patients with PAH versus controls demonstrate higher HERV-K dUTPase mRNA

Figure 4 Continued. ANOVA, analysis of variance; dUTPase, deoxyuridine triphosphate nucleotidohydrolase; HERV-K, human endogenous retrovirus K; HLADR, human leukocyte antigen-D related; IL, interleukin; pAKT, phospho-protein kinase B; PBMC, peripheral blood mononuclear cell; pERK, phospho-extracellular signal–regulated kinase; pMAPK, phospho-mitogen-activated protein kinase-activated protein kinase 2; pNFkB, phospho-nuclear factor kappa-light-chain-enhancer of activated B cells; pSTAT, phospho-signal transducer and activator of transcription; SAMHD1, SAM domain and HD domain-containing protein 1; TNF, tumor necrosis factor; and Veh, vehicle.

levels (Figure 5D), suggesting that some intrinsic factor induces higher levels of HERV-K dUTPase mRNA in PAH cells responding to an environmental or genotoxic stress. Interestingly, the differentiated ECs did not show up-regulation of HERV-K dUTPase mRNA (Figure IIE in the online-only Data Supplement). Further, no increase was discovered in HERV-K dUTPase mRNA in cultured PAH versus control PAECs (Figure IIF in the online-only Data Supplement) or PASMCs (Figure IIG in the online-only Data Supplement). This finding suggests that the propensity for HERV-K upregulation in response to an environmental stress is cell-specific.

HERV-K dUTPase Causes Pulmonary Hypertension in a Rat Model

To further substantiate a cause-and-effect relationship among HERV-K amplification, dUTPase production, and pulmonary hypertension, we delivered HERV-K dUTPase (0.2 mg/kg) by intravenous injection, once a week for 3 weeks, to adult male Sprague Dawley rats. Rats treated with HERV-K dUTPase exhibited decreased pulmonary artery acceleration time, increased right ventricular systolic blood pressure, and right ventricular hypertrophy (RVH) compared with saline-injected rats (Figure 6A through 6C). These features were associated with adverse remodeling of the pulmonary circulation judged by increased muscularization of distal PAs (Figure 6D). Cardiac output, ejection fraction, and the number of vessels per 100 alveoli in the lung were not affected by HERV-K dUTPase treatment (Figure III in the online-only Data Supplement). We further assessed the impact of HERV-K dUTPase in combination with the vascular endothelial growth factor receptor 2 blocker SU5416 (Sugen) on pulmonary hypertension in rats.[5] We observed that 3 weekly injections of HERV-K dUTPase with Sugen pretreatment resulted in increased pulmonary hypertension, as judged by a reduced pulmonary artery acceleration time, increased right ventricular systolic blood pressure and right ventricular hypertrophy, and muscularization of peripheral arteries when compared with SU5416 only-injected rats (Figure 6A through 6D).

HERV-K dUTPase induced IL6 in enriched monocytes and PAECs (Figure 4C and D). Heightened circulating levels of IL6 are observed in patients with PAH,[4] and a transgenic mouse with IL6 overexpression develops spontaneous pulmonary hypertension.[39] Indeed, rats injected intravenously with HERV-K dUTPase, with or without pretreatment with SU5416, exhibited increased IL6 by ELISA in lung tissue harvested from the rats at the

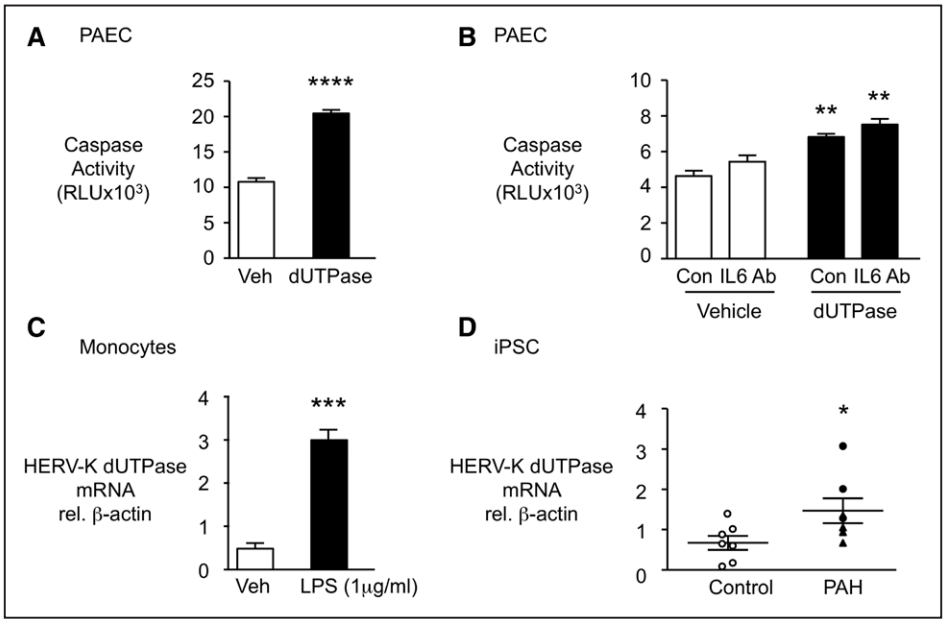

Figure 5. HERV-K dUTPase increases apoptosis in pulmonary arterial endothelial cells (PAECs) in an IL6-independent manner, is induced in monocytes by LPS and is elevated in iPSC from patients with PAH versus controls.
A, PAECs were treated with 10 μg/mL HERV-K dUTPase, and apoptosis was assessed by Caspase-Glo 3/7 assay after overnight serum withdrawal (n=4). **B,** PAECs were pretreated with neutralizing IL6 antibody (IL6 Ab) or isotype control (Con) before HERV-K dUTPase treatment (n=4). **C,** HERV-K dUTPase mRNA by qPCR in monocytes stimulated with LPS 1μg/mL (n=3). **D,** HERV-K dUTPase mRNA by qPCR in iPSC from patients with PAH (n=7) and controls (n=7). Ranges represent mean±SEM. **P*<0.05, ****P*<0.001, *****P*<0.0001 by Student's *t* test (**A, C,** and **D**). **B**, ***P*<0.01, HERV-K dUTPase versus vehicle treatment by 1-way ANOVA and post hoc Tukey test. Closed symbols (PAH), open symbols (controls), and closed triangles (hereditary PAH [HPAH]). ANOVA indicates analysis of variance; dUTPase, deoxyuridine triphosphate nucleotidohydrolase; HERV-K, human endogenous retrovirus K; IL, interleukin; iPSC, induced pluripotent stem cell; LPS, lipopolysaccharide; PAH, pulmonary arterial hypertension; qPCR, quantitative polymerase chain reaction; and RLU, relative luminescence units.

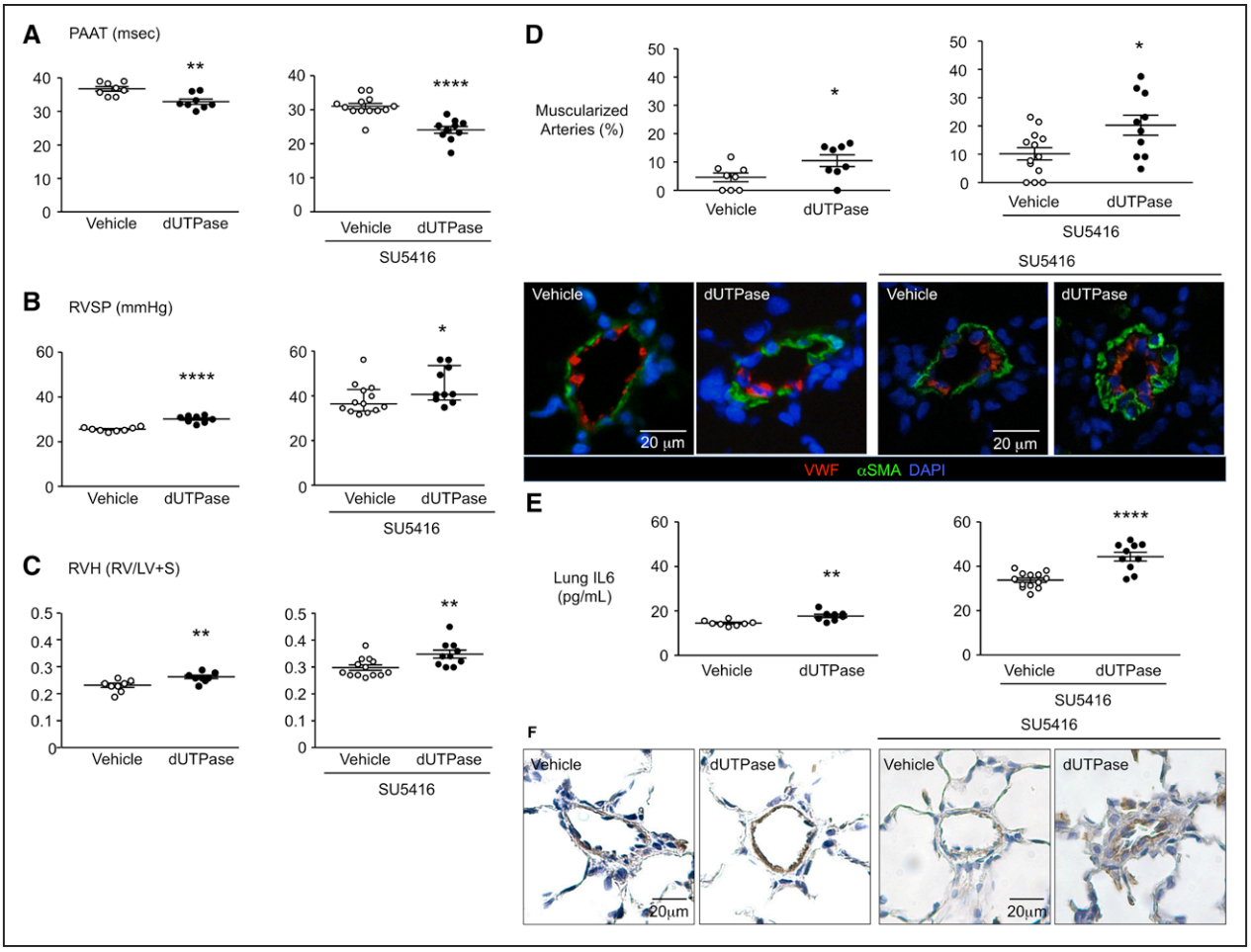

Figure 6. HERV-K dUTPase causes pulmonary hypertension in a rat.
Adult male Sprague Dawley rats (7 weeks, 180–200 g) were treated with HERV-K dUTPase (0.2 mg/kg) or saline (vehicle) once a week for 3 weeks (**left**) or were pretreated with the vascular endothelial growth factor receptor 2 blocker SU5416 (20 mg/kg) (**right**). Pulmonary and cardiac functions were evaluated on day 21. **A,** Pulmonary artery acceleration time (PAAT). **0.01, ****0.0001. **B,** Right ventricular systolic blood pressure (RVSP). *0.05, ****0.0001. **C,** Right ventricular hypertrophy (RVH). **0.01. **D,** Confocal microscopic images of lung sections of treated and control rats, immunolabeled for αSMA (green, smooth muscle cell marker), von Willebrand factor (red, endothelial cells) and nuclei (blue, 4′,6-diamidino-2-phenylindole [DAPI]) and % of muscularized distal vessels on top. *0.05. IL6 levels in lungs by enzyme-linked immunosorbent assay (**E**) and IL6 staining by IHC (**F**). **0.01, ****0.0001. Saline (n=8) or HERV-K dUTPase (n=8), SU5416 + saline (n=13), or SU5416 + HERV-K dUTPase (n=10). Ranges represent mean±SEM (**A, C, D, E,** and **B, left**) and median with interquartile range (**B, right**). *P<0.05, **P<0.01, and ****P<0.0001 by Student's t test (**A, C, D, E** and **B, left**) or by Mann Whitney test (**B, right**). dUTPase indicates deoxyuridine triphosphate nucleotidohydrolase; HERV-K, human endogenous retrovirus K; IHC, immunohistochemistry; IL, interleukin; RV/LV+S, right ventricle/left ventricle + septum; and SMA, smooth muscle actin.

end of the experimental period (Figure 6E), which was localized to PAECs and perivascular inflammatory cells (Figure 6F).

DISCUSSION

Several emerging therapies for PAH target the abnormal immune and inflammatory response linked to the pathology of PAH.[1] However, the key features that sustain immune dysregulation have not been elucidated. The identification of SAMHD1 led to the discovery of upregulation of the sequences encoding the retrovirus HERV-K and its product, dUTPase, in lungs with PAH, circulating monocytes, and iPSCs. Combined with the finding that the injection of HERV-K dUTPase induced pulmonary hypertension in a rat model, we propose that the activation of endogenous retrovirus sequences and expression of their gene products may underlie the chronic inflammatory and altered immune state associated with progressive vascular remodeling in PAH (see schema in Figure 7).

Diseases associated with HERV-K are complex diseases that probably represent the interaction of several factors, including genetic susceptibility as well as the

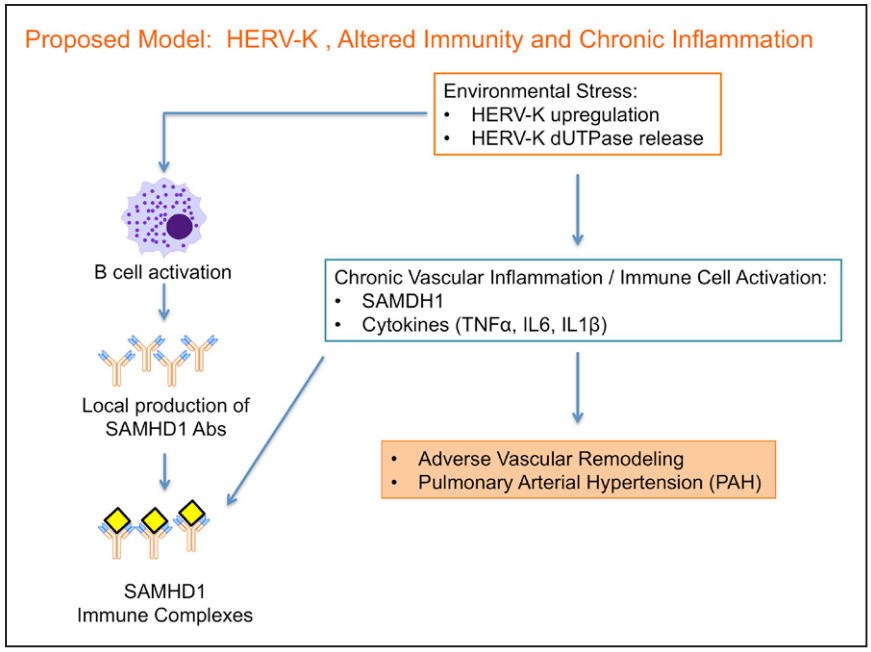

Figure 7. Proposed model for the role of HERV-K and SAMHD1 in PAH.
The endogenous retrovirus HERV-K is expanded, possibly as a result of an environmental or genotoxic stress. The product, HERV-K dUTPase, and the subsequent activation of vascular, inflammatory, and immune cells lead to adverse vascular remodeling and PAH. HERV-K, human endogenous retrovirus K; PAH, pulmonary arterial hypertension; and SAMHD1, SAM domain and HD domain-containing protein 1.

microenvironment or location of cellular injury (eg, neuronal injury may lead to the expansion of HERVs in association with multiple sclerosis).[30] Morphea, also known as localized scleroderma, is linked to the local upregulation of HERVs in skin.[40]

HIV is linked to PAH,[22] and the potential relationship between HIV as an activator of HERVs is well documented in previous studies. For example, HIV-1 Tat protein induces HERV-K mRNA, and HERV-K mRNA in PBMCs from HIV-1-infected patients is increased compared with HIV-negative controls.[41]

Although the genes associated with HERV-K are present in all cell types, they may differ in expression levels perhaps because epigenetic features and mechanisms of RNA translation can be regulated by metabolism and the cellular microenvironment.[42] In tissues from patients with PAH, high levels of HERV-K expression in perivascular CD68+ cells may be sufficient to induce paracrine effects on vascular cells and B cells that promote PAH pathology.

Cells exposed to genotoxic agents that include oxidant stress, gamma irradiation, viruses, and cytokines show an increased expression of endogenous retroviruses.[43] Genomic instability is a feature of PAH,[44] attributed to impaired DNA repair in response to a genotoxic stress,[45] that could lead to unresolved cell-specific expansion of HERV-K and sustained immune dysregulation. Lipopolysaccharide upregulated HERV-K in monocytes, and it is an environmental stress that can be genotoxic.[36] Reprogramming in iPSCs, which is known to mediate an immune response, was linked to a PAH-related increase in HERV-K. The mechanism causing the propensity for upregulation of HERV-K in certain PAH cell types would be interesting to investigate in future studies.

The expansion of HERV-K mRNA sequences has been related to both nuclear factor kappa-light-chain-enhancer of activated B cells (NFkB)-mediated transcription and a decrease in the methyltransferase SETDB1.[46] Enhanced HERV-K mRNA translation has also been described under conditions of cellular stress and is attributed to an increase in Staufin 1. Staufin 1 is a binding partner for HERV-K capsid protein, and when Staufin 1 is overexpressed, a rapid translation of HERV-K sequences occurs. Staufin 1 prevents eukaryotic initiation factor-α (EIF2α)-mediated stress granule formation, thereby facilitating mRNA translation under conditions of cellular stress.[47] This aberrant feature, impaired stress granule formation and heightened mRNA translation in response to inflammatory stress, was described by our group in PAECs with reduced bone morphogenetic protein receptor type 2,[7] owing to impaired phosphorylation of the EIF2α. It is therefore interesting that a mutation in a kinase that phosphorylates EIF2α, EIF2α kinase 4 (EIF2K4A, also known as GCN2), has been described in families with pulmonary veno-occlusive disease[48] and identified in some patients with hereditary PAH.[49]

We demonstrated that HERV-K dUTPase activates monocytes, leading to an elevated production of cytokines (tumor necrosis factor α, IL6, and IL1β) and SAMHD1. HERV-K dUTPase activates B cells in a manner that could be responsible for the local production of SAMHD1 antibodies in tertiary lymphoid tissue in lungs with PAH. Although identification of the SAMHD1 antibodies led us to the identification of HERV-K, immune complexes and the activation of complement have also been linked to PAH.[50] However, we do not know whether SAMHD1 immune complexes have heightened immunogenicity.

HERV-K dUTPase inoculation is sufficient to cause pulmonary hypertension in rats. Our model suggests a sustained effect of the dUTPase because IL6 was still elevated in the lung and localized to inflammatory and ECs 1 week after the third injection. Although a sustained elevation of IL6 levels could be responsible for pulmonary hypertension, as was seen in the transgenic IL6-overexpressing mouse,[39] other factors independent of IL6, such as those that control EC susceptibility to apoptosis, can also contribute to the pathology. It would be of interest to address the nature of endogenous retrovirus elements expressed in rodent models of pulmonary hypertension, but these elements are numerous, and a dUTPase with homology to HERV-K has not been identified.[51]

Because of the complexity of human disease, it is difficult to prove a cause-and-effect relationship rather than an association between viral infection[23,24] or endogenous retroviruses and PAH. A more comprehensive analysis of the mechanism of upregulation of retroviral sequences in PAH could lead to strategies to assess the impact of blocking the heightened production of these elements.

In summary, our findings show how upregulation of HERV-K could induce and perpetuate chronic immune dysfunction and inflammation and endothelial dysfunction, leading to adverse remodeling related to PAH.

AUTHORS

Toshie Saito, MD; Kazuya Miyagawa, MD, PhD; Shih-Yu Chen, MD, PhD; Rasa Tamosiuniene, MD, PhD; Lingli Wang, MD; Orr Sharpe, MSc; Erik Samayoa, BS, CLS; Daisuke Harada, PhD; Jan-Renier A.J. Moonen, MD, PhD; Aiqin Cao, PhD; Pin-I Chen, PhD; Jan K. Hennigs, MD; Mingxia Gu, MD, PhD; Caiyun G. Li, PhD; Ryan D. Leib, PhD; Dan Li, PhD; Christopher M. Adams, PhD; Patricia A. del Rosario, BSN, RN, PHN; Matthew Bill, BS; Francois Haddad, MD; Jose G. Montoya, MD; William H. Robinson, MD, PhD; Wendy J. Fantl, PhD; Garry P. Nolan, PhD; Roham T. Zamanian, MD; Mark R. Nicolls, MD; Charles Y. Chiu, MD, PhD; Maria E. Ariza, PhD; Marlene Rabinovitch, MD

ACKNOWLEDGMENTS

The authors greatly appreciate the editorial and technical assistance of Dr Michal Bental Roof in preparing both the article and figures, and the administrative help of Michelle Fox. T.S. and M.R. designed the experiments, analyzed and interpreted the data, and wrote the article. L.W., K.M., and R.T. helped with the animal experiments. S.-Y.C., P.-I.C., J.K.H, W.J.F., and G.P.N. assisted with single mass cytometry experiments. J.-R.A.J.M. assisted with confocal microscopic imaging and data analysis. O.S., D.H., and W.H.R. helped with experiments related to immune complex detection. E.S. and C.Y.C. performed unbiased metagenomic next-generation sequencing and computational analysis of the sequence data. M.E.A. generated and provided HERV-K dUTPase and advised on related protocols. A.C. assisted with immunoblots and ELISAs. C.G.L. assisted with the optimization of the C1q IP protocol and the initial IP analysis. R.D.L. and C.M.A. performed mass spectrometry to identify target antigens. P.A.dR., M.B., and R.T.Z. maintain the Stanford Pulmonary Hypertension Biobank and the Pulmonary Hypertension Breakthrough Initiative cell inventory, and they provided samples and clinical data for the patients with PAH. F.H. and J.G.M. obtained control samples under the same conditions. M.G. provided the iPSC and differentiated iPSC-EC. D.L. helped with immunoblots. M.R.N. critically reviewed the article.

SOURCES OF FUNDING

This work was supported by National Institutes of Health/National Heart, Lung, and Blood Institute grants N01 HV028182 (M.R., W.H.R., M.R.N., R.T.Z.), R01 HL082662 (M.R.N.), and R24 HL123767 (M.R.); National Institutes of Health/National Institute of Allergy and Infectious Diseases grant R01 A1084898 (M.E.A.); Cardiovascular Medical Research and Education Fund grant UL1 RR024986 (M.R.); and an endowed Dwight and Vera Dunlevie Chair in Pediatric Cardiology (M.R.). Mass spectrometry resources were purchased with the assistance of National Institutes of Health/National Center for Research Resources award S10RR027425. K.M. was supported by fellowships from Japan Heart Foundation/Bayer Yakuhin Research Grant Abroad and the Uehara Memorial Foundation. J.K.H. was supported by grant He 6855/1 to 1 from Deutsche Forschungsgemeinschaft. J.-R.A.J.M. is supported by The Netherlands Heart Foundation grant 2013T116. E.S. and C.Y.C. were partially supported by National Institutes of Health/National Heart, Lung, and Blood Institute grant R01 HL105704 (C.Y.C.) and research funding from Abbott Laboratories, Inc.

DISCLOSURES

None.

AFFILIATIONS

Vera Moulton Wall Center for Pulmonary Vascular Disease (T.S., K.M., R.T., L.W., J.-R.A.J.M., A.C., P.-I.C., J.K.H., M.G., C.G.L., D.L., P.A.d.R., M.B., R.T.Z., M.R.N., M.R.), Cardiovascular Institute (T.S., K.M., R.T., L.W., J.-R.A.J.M., A.C., P.-I.C., J.K.H., M.G., C.G.L., D.L., F.H., R.T.Z., M.R.N., M.R.), Department of Pediatrics (T.S., K.M., L.W., J.-R.A.J.M., A.C., P.-I.C., J.K.H., M.G., C.G.L., D.L., M.R.), Department of Microbiology and Immunology (S.-Y.C., W.J.F., G.P.N.), Baxer Laboratory for Stem Cell Biology (S.-Y.C., W.J.F., G.P.N.), Department of Medicine (R.T., O.S., D.H., P.A.d.R., M.B., F.H., J.G.M., W.H.R., R.T.Z., M.R.N.), Vincent Coates Foundation Mass Spectrometry Laboratory (R.D.L., C.M.A.), and Department of Obstetrics and Gynecology (W.J.F.), Stanford University School of Medicine, CA. Department of Laboratory Medicine and Medicine/Infectious Diseases (E.S., C.Y.C.), and Viral Diagnostics and Discovery Center University of California, San Francisco (E.S., C.Y.C.). Department of Cancer Biology and Genetics, The Ohio State University Wexner Medical Center, Columbus, OH (M.E.A.).

FOOTNOTES

Received January 25, 2017; accepted August 31, 2017.

The online-only Data Supplement is available with this article at http://circ.ahajournals.org/lookup/suppl/doi:10.1161/CIRCULATIONAHA.117.027589/-/DC1.

Circulation is available at http://circ.ahajournals.org.

REFERENCES

1. Rabinovitch M, Guignabert C, Humbert M, Nicolls MR. Inflammation and immunity in the pathogenesis of pulmonary arterial hypertension. *Circ Res*. 2014;115:165–175. doi: 10.1161/CIRCRESAHA.113.301141.
2. Dib H, Tamby MC, Bussone G, Regent A, Berezné A, Lafine C, Broussard C, Simonneau G, Guillevin L, Witko-Sarsat V, Humbert M, Mouthon L. Targets of anti-endothelial cell antibodies in pulmonary hypertension and scleroderma. *Eur Respir J*. 2012;39:1405–1414. doi: 10.1183/09031936.00181410.
3. Perros F, Dorfmüller P, Montani D, Hammad H, Waelput W, Girerd B, Raymond N, Mercier O, Mussot S, Cohen-Kaminsky S, Humbert M, Lambrecht BN. Pulmonary lymphoid neogenesis in idiopathic pulmonary arterial hypertension. *Am J Respir Crit Care Med*. 2012;185:311–321. doi: 10.1164/rccm.201105-0927OC.
4. Soon E, Holmes AM, Treacy CM, Doughty NJ, Southgate L, Machado RD, Trembath RC, Jennings S, Barker L, Nicklin P, Walker C, Budd DC, Pepke-Zaba J, Morrell NW. Elevated levels of inflammatory cytokines predict survival in idiopathic and familial pulmonary arterial hypertension. *Circulation*. 2010;122:920–927. doi: 10.1161/CIRCULATIONAHA.109.933762.
5. Tamosiuniene R, Tian W, Dhillon G, Wang L, Sung YK, Gera L, Patterson AJ, Agrawal R, Rabinovitch M, Ambler K, Long CS, Voelkel NF, Nicolls MR. Regulatory T cells limit vascular endothelial injury and prevent pulmonary hypertension. *Circ Res*. 2011;109:867–879. doi: 10.1161/CIRCRESAHA.110.236927.
6. Colvin KL, Cripe PJ, Ivy DD, Stenmark KR, Yeager ME. Bronchus-associated lymphoid tissue in pulmonary hypertension produces pathologic autoantibodies. *Am J Respir Crit Care Med*. 2013;188:1126–1136. doi: 10.1164/rccm.201302-0403OC.
7. Sawada H, Saito T, Nickel NP, Alastalo TP, Glotzbach JP, Chan R, Haghighat L, Fuchs G, Januszyk M, Cao A, Lai YJ, Perez Vde J, Kim YM, Wang L, Chen PI, Spiekerkoetter E, Mitani Y, Gurtner GC, Sarnow P, Rabinovitch M. Reduced BMPR2 expression induces GM-CSF translation and macrophage recruitment in humans and mice to exacerbate pulmonary hypertension. *J Exp Med*. 2014;211:263–280. doi: 10.1084/jem.20111741.
8. Sa S, Gu M, Chappell J, Shao NY, Ameen M, Elliott KA, Li D, Grubert F, Li CG, Taylor S, Cao A, Ma Y, Fong R, Nguyen L, Wu JC, Snyder MP, Rabinovitch M. Induced pluripotent stem cell model of pulmonary arterial hypertension reveals novel gene expression and patient specificity. *Am J Respir Crit Care Med*. 2017;195:930–941. doi: 10.1164/rccm.201606-1200OC.
9. Tojais NF, Cao A, Lai YJ, Wang L, Chen PI, Alcazar MAA, de Jesus Perez VA, Hopper RK, Rhodes CJ, Bill MA, Sakai LY, Rabinovitch M. Codependence of bone morphogenetic protein receptor 2 and transforming growth factor-β in elastic fiber assembly and its perturbation in pulmonary arterial hypertension. *Arterioscler Thromb Vasc Biol*. 2017;37:1559–1569. doi: 10.1161/ATVBAHA.117.309696.
10. Gu M, Shao NY, Sa S, Li D, Termglinchan V, Ameen M, Karakikes I, Sosa G, Grubert F, Lee J, Cao A, Taylor S, Ma Y, Zhao Z, Chappell J, Hamid R, Austin ED, Gold JD, Wu JC, Snyder MP, Rabinovitch M. Patient-specific iPSC-derived endothelial cells uncover pathways that protect against pulmonary hypertension in BMPR2 mutation carriers. *Cell Stem Cell*. 2017;20:490–504.
11. Ariza ME, Williams MV. A human endogenous retrovirus K dUTPase triggers a TH1, TH17 cytokine response: does it have a role in psoriasis? *J Invest Dermatol*. 2011;131:2419–2427. doi: 10.1038/jid.2011.217.
12. Wiśniewski JR, Zougman A, Nagaraj N, Mann M. Universal sample preparation method for proteome analysis. *Nat Methods*. 2009;6:359–362. doi: 10.1038/nmeth.1322.
13. Naccache SN, Federman S, Veeraraghavan N, Zaharia M, Lee D, Samayoa E, Bouquet J, Greninger AL, Luk KC, Enge B, Wadford DA, Messenger SL, Genrich GL, Pellegrino K, Grard G, Leroy E, Schneider BS, Fair JN, Martínez MA, Isa P, Crump JA, DeRisi JL, Sittler T, Hackett J Jr, Miller S, Chiu CY. A cloud-compatible bioinformatics pipeline for ultrarapid pathogen identification from next-generation sequencing of clinical samples. *Genome Res*. 2014;24:1180–1192. doi: 10.1101/gr.171934.113.
14. Pavlidis P, Noble WS. Matrix2png: a utility for visualizing matrix data. *Bioinformatics*. 2003;19:295–296. https://doi.org/10.1093/bioinformatics/19.2.295.
15. Bendall SC, Simonds EF, Qiu P, Amir el-AD, Krutzik PO, Finck R, Bruggner RV, Melamed R, Trejo A, Ornatsky OI, Balderas RS, Plevritis SK, Sachs K, Pe'er D, Tanner SD, Nolan GP. Single-cell mass cytometry of differential immune and drug responses across a human hematopoietic continuum. *Science*. 2011;332:687–696. doi: 10.1126/science.1198704.
16. Roxas BA, Li Q. Significance analysis of microarray for relative quantitation of LC/MS data in proteomics. *BMC Bioinformatics*. 2008;9:187. doi: 10.1186/1471-2105-9-187.
17. Gaudillière B, Fragiadakis GK, Bruggner RV, Nicolau M, Finck R, Tingle M, Silva J, Ganio EA, Yeh CG, Maloney WJ, Huddleston JI, Goodman SB, Davis MM, Bendall SC, Fantl WJ, Angst MS, Nolan GP. Clinical recovery from surgery correlates with single-cell immune signatures. *Sci Transl Med*. 2014;6:255ra131. doi: 10.1126/scitranslmed.3009701.
18. Kretschmer S, Wolf C, König N, Staroske W, Guck J, Häusler M, Luksch H, Nguyen LA, Kim B, Alexopoulou D, Dahl A, Rapp A, Cardoso MC, Shevchenko A, Lee-Kirsch MA. SAMHD1 prevents autoimmunity by maintaining genome stability. *Ann Rheum Dis*. 2015;74:e17. doi: 10.1136/annrheumdis-2013-204845.
19. Goldstone DC, Ennis-Adeniran V, Hedden JJ, Groom HC, Rice GI, Christodoulou E, Walker PA, Kelly G, Haire LF, Yap MW, de Carvalho LP, Stoye JP, Crow YJ, Taylor IA, Webb M. HIV-1 restriction factor SAMHD1 is a deoxynucleoside triphosphate triphosphohydrolase. *Nature*. 2011;480:379–382. doi: 10.1038/nature10623.
20. Aloisi F, Pujol-Borrell R. Lymphoid neogenesis in chronic inflammatory diseases. *Nat Rev Immunol*. 2006;6:205–217. doi: 10.1038/nri1786.
21. Sze A, Olagnier D, Lin R, van Grevenynghe J, Hiscott J. SAMHD1 host restriction factor: a link with innate immune sensing of retrovirus infection. *J Mol Biol*. 2013;425:4981–4994. doi: 10.1016/j.jmb.2013.10.022.
22. Flores SC, Almodovar S. Human immunodeficiency virus, herpes virus infections, and pulmonary vascular disease. *Pulm Circ*. 2013;3:165–170. doi: 10.4103/2045-8932.109955.
23. Cool CD, Rai PR, Yeager ME, Hernandez-Saavedra D, Serls AE, Bull TM, Geraci MW, Brown KK, Routes JM, Tuder RM, Voelkel NF. Expression of human herpesvirus 8 in primary pulmonary hypertension. *N Engl J Med*. 2003;349:1113–1122. doi: 10.1056/NEJMoa035115.
24. Demir C, Demir M. Effect of hepatitis C virus infection on the right ventricular functions, pulmonary arterypressure and pulmonary vascular resistance. *Int J Clin Exp Med*. 2014;7:2314–2318.
25. Valmary S, Dorfmüller P, Montani D, Humbert M, Brousset P, Degano B. Human γ-herpesviruses Epstein-Barr virus and human herpesvirus-8 are not detected in the lungs of patients with severe pulmonary arterial hypertension. *Chest*. 2011;139:1310–1316. doi: 10.1378/chest.10-1200.
26. Chiu CY. Viral pathogen discovery. *Curr Opin Microbiol*. 2013;16:468–478. doi: 10.1016/j.mib.2013.05.001.
27. Hohn O, Hanke K, Bannert N. HERV-K(HML-2), the best preserved family of HERVs: endogenization, expression, and implications in health and disease. *Front Oncol*. 2013;3:246. doi: 10.3389/fonc.2013.00246.
28. Grow EJ, Flynn RA, Chavez SL, Bayless NL, Wossidlo M, Wesche DJ, Martin L, Ware CB, Blish CA, Chang HY, Pera RA, Wysocka J. Intrinsic retroviral reactivation in human preimplantation embryos and pluripotent cells. *Nature*. 2015;522:221–225. doi: 10.1038/nature14308.
29. Johanning GL, Malouf GG, Zheng X, Esteva FJ, Weinstein JN, Wang-Johanning F, Su X. Expression of human endogenous retrovirus-K is strongly associated with the basal-like breast cancer phenotype. *Sci Rep*. 2017;7:41960. doi: 10.1038/srep41960.
30. Perron H, Bernard C, Bertrand JB, Lang AB, Popa I, Sanhadji K, Portoukalian J. Endogenous retroviral genes, Herpesviruses and gender in Multiple Sclerosis. *J Neurol Sci*. 2009;286:65–72. doi: 10.1016/j.jns.2009.04.034.
31. Pullmann R Jr, Bonilla E, Phillips PE, Middleton FA, Perl A. Haplotypes of the HRES-1 endogenous retrovirus are associated with development and disease manifestations of systemic lupus erythematosus. *Arthritis Rheum*. 2008;58:532–540. doi: 10.1002/art.23161.
32. Freimanis G, Hooley P, Ejtehadi HD, Ali HA, Veitch A, Rylance PB, Alawi A, Axford J, Nevill A, Murray PG, Nelson PN. A role for human endogenous retrovirus-K (HML-2) in rheumatoid arthritis: investigating mechanisms of pathogenesis. *Clin Exp Immunol*. 2010;160:340–347. doi: 10.1111/j.1365-2249.2010.04110.x.
33. Foerster J, Nolte I, Junge J, Bruinenberg M, Schweiger S, Spaar K, van der Steege G, Ehlert C, Mulder M, Kalscheuer V, Blumenthal-Barby E, Win-

ter J, Seeman P, Ständer M, Sterry W, Te Meerman G. Haplotype sharing analysis identifies a retroviral dUTPase as candidate susceptibility gene for psoriasis. *J Invest Dermatol*. 2005;124:99–102. doi: 10.1111/j.0022-202X.2004.23504.x.

34. Lai OY, Chen H, Michaud HA, Hayashi G, Kuebler PJ, Hultman GK, Ariza ME, Williams MV, Batista MD, Nixon DF, Foerster J, Bowcock AM, Liao W. Protective effect of human endogenous retrovirus K dUTPase variants on psoriasis susceptibility. *J Invest Dermatol*. 2012;132:1833–1840. doi: 10.1038/jid.2012.69.
35. Berglund LJ, Avery DT, Ma CS, Moens L, Deenick EK, Bustamante J, Boisson-Dupuis S, Wong M, Adelstein S, Arkwright PD, Bacchetta R, Bezrodnik L, Dadi H, Roifman CM, Fulcher DA, Ziegler JB, Smart JM, Kobayashi M, Picard C, Durandy A, Cook MC, Casanova JL, Uzel G, Tangye SG. IL-21 signalling via STAT3 primes human naive B cells to respond to IL-2 to enhance their differentiation into plasmablasts. *Blood*. 2013;122:3940–3950. doi: 10.1182/blood-2013-06-506865.
36. Cavallo P, Cianciulli A, Mitolo V, Panaro MA. Lipopolysaccharide (LPS) of helicobacter modulates cellular DNA repair systems in intestinal cells. *Clin Exp Med*. 2011;11:171–179. doi: 10.1007/s10238-010-0118-1.
37. Lee J, Sayed N, Hunter A, Au KF, Wong WH, Mocarski ES, Pera RR, Yakubov E, Cooke JP. Activation of innate immunity is required for efficient nuclear reprogramming. *Cell*. 2012;151:547–558. doi: 10.1016/j.cell.2012.09.034.
38. Ohnuki M, Tanabe K, Sutou K, Teramoto I, Sawamura Y, Narita M, Nakamura M, Tokunaga Y, Nakamura M, Watanabe A, Yamanaka S, Takahashi K. Dynamic regulation of human endogenous retroviruses mediates factor-induced reprogramming and differentiation potential. *Proc Natl Acad Sci U S A*. 2014;111:12426–12431. doi: 10.1073/pnas.1413299111.
39. Steiner MK, Syrkina OL, Kolliputi N, Mark EJ, Hales CA, Waxman AB. Interleukin-6 overexpression induces pulmonary hypertension. *Circ Res*. 2009;104:236–244. doi: 10.1161/CIRCRESAHA.108.182014.
40. Kowalczyk MJ, Dańczak-Pazdrowska A, Szramka-Pawlak B, Zaba R, Silny W, Osmola-Mańkowska A. Expression of selected human endogenous retroviral sequences in skin and peripheral blood mononuclear cells in morphea. *Arch Med Sci*. 2012;8:819–825. doi: 10.5114/aoms.2012.30954.
41. Bhardwaj N, Maldarelli F, Mellors J, Coffin JM. HIV-1 infection leads to increased transcription of human endogenous retrovirus HERV-K (HML-2) proviruses *in vivo* but not to increased virion production. *J Virol*. 2014;88:11108–11120. doi: 10.1128/JVI.01623-14.
42. Okahara G, Matsubara S, Oda T, Sugimoto J, Jinno Y, Kanaya F. Expression analyses of human endogenous retroviruses (HERVs): tissue-specific and developmental stage-dependent expression of HERVs. *Genomics*. 2004;84:982–990. doi: 10.1016/j.ygeno.2004.09.004.
43. Wu Y, Qi X, Gong L, Xing G, Chen M, Miao L, Yao J, Suzuki T, Furihata C, Luan Y, Ren J. Identification of BC005512 as a DNA damage responsive murine endogenous retrovirus of GLN family involved in cell growth regulation. *PLoS One*. 2012;7:e35010. doi: 10.1371/journal.pone.0035010.
44. Aldred MA, Comhair SA, Varella-Garcia M, Asosingh K, Xu W, Noon GP, Thistlethwaite PA, Tuder RM, Erzurum SC, Geraci MW, Coldren CD. Somatic chromosome abnormalities in the lungs of patients with pulmonary arterial hypertension. *Am J Respir Crit Care Med*. 2010;182:1153–1160. doi: 10.1164/rccm.201003-0491OC.
45. Li M, Vattulainen S, Aho J, Orcholski M, Rojas V, Yuan K, Helenius M, Taimen P, Myllykangas S, De Jesus Perez V, Koskenvuo JW, Alastalo TP. Loss of bone morphogenetic protein receptor 2 is associated with abnormal DNA repair in pulmonary arterial hypertension. *Am J Respir Cell Mol Biol*. 2014;50:1118–1128. doi: 10.1165/rcmb.2013-0349OC.
46. Collins PL, Kyle KE, Egawa T, Shinkai Y, Oltz EM. The histone methyltransferase SETDB1 represses endogenous and exogenous retroviruses in B lymphocytes. *Proc Natl Acad Sci U S A*. 2015;112:8367–8372. doi: 10.1073/pnas.1422187112.
47. Hanke K, Hohn O, Liedgens L, Fiddeke K, Wamara J, Kurth R, Bannert N. Staufen-1 interacts with the human endogenous retrovirus family HERV-K(HML-2) rec and gag proteins and increases virion production. *J Virol*. 2013;87:11019–11030. doi: 10.1128/JVI.03031-12.
48. Eyries M, Montani D, Girerd B, Perret C, Leroy A, Lonjou C, Chelghoum N, Coulet F, Bonnet D, Dorfmüller P, Fadel E, Sitbon O, Simonneau G, Tregouët DA, Humbert M, Soubrier F. EIF2AK4 mutations cause pulmonary veno-occlusive disease, a recessive form of pulmonary hypertension. *Nat Genet*. 2014;46:65–69. doi: 10.1038/ng.2844.
49. Hadinnapola C, Bleda M, Haimel M, Screaton N, Swift AJ, Dorfmüller P, Preston SD, Southwood M, Hernandez-Sanchez J, Martin J, Treacy C, Yates K, Bogaard H, Church C, Coghlan G, Condliffe R, Corris PA, Gibbs SR, Girerd B, Holden S, Humbert M, Kiely DG, Lawrie A, Machado RD, MacKenzie Ross R, Moledina S, Montani D, Newnham M, Peacock AJ, Pepke-Zaba J, Rayner-Matthews PJ, Shamardina O, Soubrier F, Southgate L, Suntharalingam J, Toshner MR, Trembath RC, Vonk Noordegraaf A, Wilkins MR, Wort SJ, Wharton J, Gräf S, Morrell NW; NIHR BioResource - Rare Diseases Consortium & UK National Cohort Study of Idiopathic and Heritable PAH. Phenotypic characterisation of EIF2AK4 mutation carriers in a large cohort of patients diagnosed clinically with pulmonary arterial hypertension [published online ahead of print September 28, 2017]. *Circulation*. doi: 10.1161/CIRCULATIONAHA.117.028351.
50. Bauer EM, Zheng H, Comhair S, Erzurum S, Billiar TR, Bauer PM. Complement C3 deficiency attenuates chronic hypoxia-induced pulmonary hypertension in mice. *PLoS One*. 2011;6:e28578. doi: 10.1371/journal.pone.0028578.
51. Garcia-Etxebarria K, Jugo BM. Genome-wide reexamination of endogenous retroviruses in Rattus norvegicus. *Virology*. 2016;494:119–128. doi: 10.1016/j.virol.2016.04.006.

Upregulation of Human Endogenous Retrovirus-K Is Linked to Immunity and Inflammation in Pulmonary Arterial Hypertension

Toshie Saito, Kazuya Miyagawa, Shih-Yu Chen, Rasa Tamosiuniene, Lingli Wang, Orr Sharpe, Erik Samayoa, Daisuke Harada, Jan-Renier A.J. Moonen, Aiqin Cao, Pin-I Chen, Jan K. Hennigs, Mingxia Gu, Caiyun G. Li, Ryan D. Leib, Dan Li, Christopher M. Adams, Patricia A. del Rosario, Matthew Bill, Francois Haddad, Jose G. Montoya, William H. Robinson, Wendy J. Fantl, Garry P. Nolan, Roham T. Zamanian, Mark R. Nicolls, Charles Y. Chiu, Maria E. Ariza and Marlene Rabinovitch

Circulation. 2017;136:1920-1935; originally published online September 21, 2017;
doi: 10.1161/CIRCULATIONAHA.117.027589
Circulation is published by the American Heart Association, 7272 Greenville Avenue, Dallas, TX 75231

Print ISSN: 0009-7322. Online ISSN: 1524-4539

SUPPLEMENTAL MATERIAL

Upregulation of HERV-K is Linked to Immunity and Inflammation in Pulmonary Arterial Hypertension

Toshie Saito, Kazuya Miyagawa, Shih-Yu Chen, Rasa Tamosiuniene, Lingli Wang, Orr Sharpe, Erik Samayoa, Daisuke Harada, Jan-Renier A. J. Moonen, Aiqin Cao, Pin-I Chen, Jan K. Hennigs, Mingxia Gu, Caiyun G. Li, Ryan D. Leib, Dan Li, Christopher M. Adams, Patricia A. del Rosario, Matthew Bill, Francois Haddad, Jose G. Montoya, William H. Robinson, Wendy J. Fantl, Garry P. Nolan, Roham T. Zamanian, Mark R. Nicolls, Charles Y. Chiu, Maria E. Ariza, Marlene Rabinovitch

Expanded Methods:

Human samples (lung tissue and peripheral blood mononuclear cells, pulmonary artery endothelial cells (PAEC), pulmonary artery smooth muscle cells (PASMC), induced pluripotent stem cells (iPSC), iSPC differentiated into endothelial cells (iPSC-EC) from PAH patients and donor controls

Procurement of the tissues from human subjects was approved by the Administrative Panel on Human Subjects in Medical Research at the PHBI Transplant Procurement Centers (lung tissues) and at Stanford University (for blood) and at Vanderbilt University courtesy of Dr. Eric Austin for some of the fibroblasts used for induced pluripotent stem cells. Written informed consent was received from participants prior to inclusion in the study. Characteristics of PAH patients and healthy controls used in the various studies are provided in Supplemental Tables 1 and 2.

Lungs (PAH and donor controls): Lung tissues from heredity and idiopathic PAH patients and control subjects (unused donor lungs) were provided by the Pulmonary Hypertension Breakthrough Initiative (PHBI), which is funded by NIH/NHLBI and the Cardiovascular Medical Research and Education Fund (CMREF). The tissues were obtained from the PHBI Transplant Procurement Centers at Allegheny Hospital, Pittsburgh, PA, Baylor University, The Cleveland Clinic, Stanford University, University of Alabama at Birmingham, The University of California, San Diego, University of Michigan, and Vanderbilt University and de-identified patient data were obtained via the PHBI Data Coordinating Center at the University of Michigan. The lungs were

processed and stored as described previously[1]. In brief, lung tissues were kept in DMEM media supplemented with antibiotics for up to 24h during transportation from the transplant procurement centers. Small pieces of lung tissues were snap-frozen in liquid nitrogen and stored at -80^{o}C for biochemical experiments or fixed in 10% formaldehyde overnight for immunohistochemistry.

Pulmonary artery endothelial cells (PAEC), pulmonary artery smooth muscle cells (PASMC), induced pluripotent stem cells (iPSC) and induced pluripotent stem cells differentiated into endothelial cells (iPSC-EC): Most of the cells were obtained from PAH and control (unused donor) lungs provided by PHBI network. The cells were harvested using standard protocols previously published[2,3] Some of the fibroblasts used for induced pluripotent stem cells were obtained from Vanderbilt University as described before[2,4].

Peripheral blood mononuclear cells (PBMC): PBMC were isolated from blood of PAH patients, provided by the Stanford Human Immune Monitoring Center (HIMC) Biobank (Director: Dr. Gupta; in collaboration with Dr. Zamanian), and from blood of healthy donors, provided by Dr. Montoya. Additional PBMC for the HERV-K dUTPase experiments (experimental samples and assay controls) were isolated from blood obtained from the Stanford Blood Center.

Cell isolation and culture

PAH patient and control cells were obtained described above. Primary pulmonary arterial endothelial cells (PAEC) were also obtained from PromoCell (Heidelberg, Germany). PAEC were cultured in EC media supplemented with 5% fetal bovine serum (FBS), EC growth supplement and penicillin/streptomycin (ScienCell, Carlsbad, CA) and used at passage 3-6. PASMC were cultured in smooth muscle cell media supplemented with 5% fetal bovine serum (FBS), SMC growth supplement and gentamaicin/amphotericin-B (Lonza, Basel, Switzerland) and used at passage 4-10. iPSC and iPS-EC were cultured as described before[4]. PBMC were separated by Ficoll-Paque (GE Healthcare, Pittsburgh, PA) following centrifugation of whole blood at 400 g for 30 min. PBMC ($1X10^7$) were used for further preparation of enriched monocytes. Cells that attached to wells after two hours represented an enriched monocyte preparation. For detection of HERV-K dUTPase in monocytes by qPCR, we used the Pan Monocyte Isolation kit (Miltenyi Biotec, Auburn, CA), according to the manufacturer's protocol. PBMC were cultured with RPMI-1640 (ATCC, Manassas, VA), supplemented with 10% FBS and penicillin/streptomycin.

HERV-K dUTPase protein purification

Recombinant HERV-K dUTPase protein was provided by Dr. Ariza. The herv-k gene encoding the dUTPase was cloned into the pTrcHis Topo TA expression vector and the sequence verified by DNA sequencing analysis, as previously described[5]. The purity of the protein was assessed by SDS-PAGE and capillary-liquid chromatography nanospray tandem mass spectrometry (nano-LC/MSMS) performed at the Ohio State

University Mass Spectrometry and Proteomics Facility. Purified dUTPase preparations were routinely tested for contaminating DNA, RNA, lipopolysaccharide and peptidoglycan as previously described[5] to ensure high purity.

Treatment of cells with HERV-K dUTPase recombinant protein

PAEC ($1x10^6$), PBMCs ($1x10^6$), or enriched monocytes (isolated from $1x10^7$ PBMCs as described above) were used. Cells were incubated with 0.1, 1.0, or 10 μg/ml of recombinant HERV-K dUTPase for 24 hr. Supernatants were collected and used for cytokine measurement by ELISA, and cell lysates were used for western immunoblotting. PBMC were analyzed by single mass cytometry (CyTOF). PAEC were also assed for apoptosis judged by heightened caspase activity (Caspase-Glo 3/&) (Promega, Madison, WI) during serum withdrawal for 16hrs[2]. PASMC were assed for proliferation (MTT proliferation assay, ATCC, Manassas, VA)[6] in response to HERV-K dUTPase for 48 hr.

Caspase assay

Survival of PAEC was assessed by the Caspase 3/7 assay. In some experiments, IL-6 neutralizing antibody (InvioGen, San Diego, CA) vs. Isotype control (InvioGen, San Diego, CA) was used to assess whether PAEC apoptosis induced by HERV-K was IL-6 dependent.

Monoculture of PAEC: PAEC ($8X10^3$) were seeded in 96-well plate with 5% FBS and allowed to adhere overnight. Cells were incubated with 10 μg/ml of recombinant

HERV-K dUTPase in FBS free media for 16 hr. Cells were assessed with Caspase 3/7 Luciferase Reagent Mix (Promega, Madison, WI), according to the manufacturer's protocol.

Co-culture of PAEC and Monocytes: PAEC ($1X10^5$) were seeded in 12-well plates with 5% FBS and allowed to adhere overnight. Pan Monocyte Isolation kit (Miltenyi Biotec, Auburn, CA) was used to isolated monocytes as described above. Then $5X10^5$ monocytes were pre-treated on a cell culture insert with 10 μg/ml of recombinant HERV-K dUTPase for 2 hr. Then the monocytes were added to the PAEC cultures for 8 hr. After co-culture, the cell culture insert (monocytes) was removed, media of PAEC were changed to serum free media and incubated for 16 hr. Cells were assessed with Caspase 3/7 Luciferase Reagent Mix (Promega, Madison, WI), according to the manufacturer's protocol.

MTT Assay

Proliferation of PASMC was assessed by MTT. PASMC ($8X10^3$) were seeded in 96-well plates with 5% FBS and allowed to adhere overnight. Cells were incubated with 10 μg/ml of recombinant HERV-K dUTPase in 5% FBS media for 48 hr. Cells were assessed with MTT (ATCC, Manassas, VA), according to the manufacturer's protocol.

Treatment with lipopolysaccharide (LPS)

Monocytes and PAEC cultured as described above were treated with 1 μg/ml LPS for 6 hr and cell lysates were used to asses HERV-K dUTPase mRNA by qPCR.

Immunohistochemistry

Lung tissue sections (approx. 1.2 cm x 1.2 cm) were fixed with 10% formaldehyde (Thermo Scientific, Waltham, MA) and embedded in paraffin (Leica Biosystem, Buffalo Grove, IL). After deparaffinization, sections were permeabilized with 0.2% Triton (Sigma Aldrich, St. Louis, MO). Antigen retrieval was done with either citrate buffer pH 6.0 (Sigma Aldrich, St. Louis, MO) or 1 mM EDTA pH 8.0 (Life Technologies, Grand Island, NY), depending on the primary antibodies. Sections were immersed in 0.3% hydrogen peroxide (Sigma Aldrich, St. Louis, MO) to prevent endogenous peroxidase activity, blocked with 5% goat serum (Jackson ImmunoResearch, West Grove, PA) and incubated with primary antibodies overnight at 4^{o}C, or for one hour at room temperature, depending on the primary antibodies. The following primary antibodies were used: SAMHD1 (1:500, Abcam), CD3 (1:50, Dako), CD19 (1:100, Dako), Plasma Cell (1:100 Dako), Follicular Dendritic cell (FDC) (1:50, Dako), IL6 (1:1000, Abcam). After incubation with secondary antibodies for one hour at RT and amplification with streptavidin-biotin (LSAB2 kit, DAKO, Carpinteria, CA), sections were stained with 3,3-diaminobenzidine (DAB) and (LSAB2 kit, DAKO, Carpinteria, CA) counterstained with hematoxylin (Vector Laboratories, Burlingame, CA). Images were acquired using a Leica DMLB microscope (Leica, Buffalo Grove, IL).

Quantification of SAMHD1 staining: Six PAs and associated perivascular regions were randomly chosen for each sample. SAMHD1-immunestained nuclei were evaluated by the ImmunoRatio[7], a publicly available automated web-based image analysis program. We used the program to calculate the percentage of DAB-stained

SAMHD1 positive nuclear area relative to the total nuclear area. The average values of six PAs for each sample are shown.

Quantification of tertiary lymphoid tissue: Tertiary lymphoid tissue was evaluated by H&E and T cell, B cell, plasma cell and follicular dendritic cell markers. The ratio of PAs with tertiary lymphoid tissue relative to the total number of PAs in each sample was calculated and shown as % of total for each patient and each control.

Immunofluorescent staining

Lung sections (approx. 1.2 cm X 1.2 cm) were fixed with 10% formaldehyde (Thermo Scientific, Waltham, MA) and embedded in paraffin (Leica Biosystem, Buffalo Grove, IL). After deparaffinization, sections were permeabilized with 0.2% Triton (Sigma Aldrich, St. Louis, MO). Antigen retrieval was done with either citrate buffer pH 6.0 (Sigma Aldrich, St. Louis, MO) or 1 mM EDTA pH 8.0 (Life Technologies, Grand Island, NY), depending on the primary antibodies. Sections were blocked with 5% goat serum (Jackson ImmunoResearch, West Grove, PA) and incubated with primary antibodies overnight at 4^{o}C, or for one hour at room temperature, depending on the primary antibodies. The following primary antibodies were used: SAMHD1 (1:500, Abcam), VVF (1:1000, Abcam), CD11c (1:100, Abcam), CD68 (1:100, Dako), CD3 (1:50, Dako), HERV-K env (1:1000, Austral), HERV-K dUTPase (1:2000, provided by Dr. Ariza), α-Actin (1:400, Sigma Aldrich), followed by incubation with fluorophore-conjugated secondary antibodies (Alexa Fluor 488 anti mouse and Alexa Fluor 594 anti rabbit) for one hour at RT. When double staining with the primary antibodies from same species

was done, Zenon kit (Life technologies, Grand Island, NY) was used for direct labeling of primary antibodies with fluorophores, according to the manufacturer's protocol. Nuclei were stained with DAPI (Vector Laboratories, Burlingame, CA). Images were acquired using a FlouView 1000 (Olympus, Center Valley, PA) or a Leica TCS SP8 (Leica, Buffalo Grove, IL) confocal microscope.

In situ SAMHD1 antibody production

To localize SAMHD1 antibody producing cells, frozen lung tissues were fixed with acetone (Sigma Aldrich, St. Louis, MO), blocked with 5% normal goat serum (Jackson ImmunoResearch, West Grove, PA) and incubated with GST-tagged SAMHD1 recombinant protein (Novus Biologicals, Littleton, CO) in PBS (20 μg/ml) overnight at 4˚C. Sections were washed with PBS and incubated with FITC-conjugated anti GST antibody (Abcam, 1:800) for one hour at RT. Nuclei were stained with DAPI (Vector Laboratories, Burlingame, CA). Images were acquired using a FlouView 1000 (Olympus, Center Valley, PA) confocal microscope.

Immune complex immunoprecipitation and mass spectrometry to identify target antigens

Immune complexes were captured using a Direct IP kit (Life Technologies, Grand Island, NY), according to the manufacturer's protocol. In brief, 10 μg of C1q (Sigma, St. Louis, MO) was coupled to AminoLink Plus Coupling Resin (Life Technologies, Grand Island, NY). Lung tissue (100mg) was lysed using a dounce homogenizer and 500 μl of lysis buffer (0.025 M Tris HCl pH 7.5, 0.15 M NaCl, 1 mM EDTA, 0.5% NP40,

5% glycerol) with proteinase/phosphatase inhibitors (Life Technologies, Grand Island, NY). After centrifugation at 20,000 g for 20 min at 4˚C, the supernatant was collected. The lysates were incubated with C1q coupled resin overnight at 4˚C. After the incubation, the beads were washed four times and eluted with 50 μl of IgG Elution Buffer (Life Technologies, Grand Island, NY) for 10 min using gentle vortex and neutralizes with 1 M Tris-HCl pH 9.0. The samples were then prepared using filter aided sample preparation (FASP)[8]. In brief, solubilized proteins in a 4% SDS, 0.1 M DTT, 0.1 M Tris-HCl pH 7.8 were exchanged into first an 8 M urea containing buffer, followed by a 50 mM ammonium bicarbonate buffer on an ultracentrifuge filter. Following a buffer exchange, digestion using trypsin was performed on the membrane filter overnight at 37˚C, where peptides were spun out, collected and further cleaned on C18 reverse phase material and analyzed by liquid chromatography (LC) and mass spectrometry (MSMS).

The LC was a NanoLC-2D (Eksigent) where mobile phase A was 99.9% water, 0.1% formic acid and mobile phase B was 99.9% acetonitrile, 0.1% formic acid run at a flow rate of 600 nL/min. The reversed phase C18 column was packed in-house using PEEKE C18 3 μM material to a length of 15 cm where the column inner diameter was 100 μM. The source was a Michrom-Bruker Advance Captive Spray with an electrospray potential of 1.7 kV. The mass spectrometer was a LTQ Orbitrap Velos set in data dependent acquisition (DDA) mode, to isolate and fragment the top 12 most intense multiply charged precursor ions. The raw data were converted to .mgf format and searched by Byonic (Protein Metrics) using typical search conditions and a

1% False Discovery Rate determined using the standard reverse decoy strategy. Byonic output files were further analyzed using custom scripts developed in Matlab to aid in data visualization. We excluded proteins where we did not observe at least 3 peptides in at least one sample. Common contaminants were also excluded. For all other proteins, control and PAH patient data were assed using significance analysis of microarray (SAM) to determine q values with a false discovery rate (FDR) cutoff of 5%[9].

Quantification of SAMHD1 specific Immune complexes

Lung tissue (100 mg) was lysed using a dounce homogenizer and 500 μl of lysis buffer (0.025 M Tris-HCl pH 7.5, 0.15 M NaCl, 1 mM EDTA, 0.5% NP40, 5% glycerol) with proteinase/phosphatase inhibitors (Life Technologies, Grand Island, NY). After centrifugation at 20,000 g for 20 min at 4˚C, total protein concentration of the supernatant was measured and diluted in PBS to 1 μg/μl total protein. ELISA plates were coated with 0.02 mg/mL SAMHD1 antibody (Abcam) in PBS overnight at 4˚C. The plates were blocked with 5% BSA in PBS for one hour. Lung lysate was applied and incubated for two hours. HRP-conjugated species-specific anti human IgG (GE Healthcare, 1:10000) added to the plates, and incubated for one hour at room temperature. Tetramethylbenzidine substrate (R&D, Minneapolis, MN) was added for 15 min, then the reaction was stopped with 2 N sulfuric acid (R&D, Minneapolis, MN), and OD values were determined at 450 nm.

Western immunoblotting

Lung lysates (50 mg) were prepared by homogenization with 500 μl of modified RIPA buffer (50 mM Tris-HCl pH 7.4, 150 mM NaCl, 1 mM EDTA, 1% Triton X-100, 0.1% SDS, 1% Sodium deoxycholate, 1 mM PMSF) containing protease and phosphatase inhibitors (Life Technologies, Grand Island, NY). After centrifugation at 20,000 g for 20 min at 4˚C, the supernatant was collected. Protein concentration was determined by BCA. Equal amounts of protein were loaded on a precast NuPage 4-12% Bis-Tris (LifeTechnologies) gel and subjected to electrophoresis under reducing conditions and electrotransferred onto polyvinylidene difluoride (PVDF) membranes. After blocking with 5% milk in 0.5% Tween-PBS, membranes were incubated with primary antibodies against SAMHD1 (1:500, Abcam), pSTAT3 (1:1000, Invitrogen), STAT3 (1:1000, Invitrogen), β-Actin (1:10000, Santa Cruz Biotechnology), α-Tubulin (1:2000, Sigma Aldrich). Anti mouse IgG secondary antibody (1:5000, Santa Cruz Biotechnology) was used. After incubation with HRP-conjugated secondary antibodies, signals were visualized with ECL or ECL prime (GE Healthcare, Pittsburgh, PA).

Enzyme-linked immunosorbent assay (ELISA)

Cytokine levels in human enriched monocytes, human PAEC, and rat lung lysates were measured using the Quantikine ELISA kit (R&D, Minneapolis, MN) for human TNFα, IL1β and IL6, and for rat IL6 (LSBio, Seattle, WA), according to the manufacturer's protocol.

Quantitative (q)PCR

Total RNA was extracted and purified from lung tissue or cells using spin column based kits (Qiagen, Valencia, CA, or Zymo Research, Irvine, CA). RT-PCR was performed according to the manufacture's protocol (Applied Biosystems, Grand Island, NY). qPCR was performed with a 7900HT Sequence Detection System (Applied Biosystems, Foster, CA) or a CFX384 Real Time System (BioRad, Hercules, CA). Primers used: TaqMan Gene Expression Assays, (β-actin (Hs01060665_g1), HERV-K(II) env (PN4441114, custom probe, Applied Biosystems) and Syber Green assays, HERV-K dUTPase (Forward, 5'-AAATGGGCAACCATTGTCGGGAAACGAGC-3'; Reverse, 5'-TAGTACAT AAATCTACTGCTGCACTGC-3), β-actin (Forward,5'-CATGCCATCCTGCGTCTGGA-3'; Reverse, 5'-CCGTGGCCATCTCTTGCTCG).

Unbiased pan-viral metagenomic next-generation sequencing

A 0.5 cm^3 piece of previously snap frozen lung tissue was placed in a 2 mL tube with RLT Buffer (Qiagen, Hilden, Germany) and 0.1 mm silica beads (MPBiomedicals, Solon OH). Next, the samples were homogenized using an Omni Bead Ruptor (Omni Intl, Kennesaw, GA), and cellular debris was pelleted. Total RNA was extracted using the EZ1 RNA Universal Tissue kit (Qiagen, Hilden, Germany). An on-instrument DNase treatment was performed to minimize any background genomic DNA, followed by enrichment for polyadenylated mRNA using OligoTex (Qiagen, Hilden, Germany). Nucleic acid samples were randomly amplified to generate a cDNA library as previously described[10], and the quality and size distributions of the libraries were examined by 2% agarose gel electrophoresis. Metagenomic sequencing libraries were then generated

using a modified Illumina TruSeq protocol[10]. The BioAnalyzer High-Sensitivity DNA kit (Agilent, Santa Clara, CA) was used to assess library size and the Kapa Universal qPCR kit (Kapa Biosystems, Woburn, MA) was used to quantitate the library concentration. After validation, samples were sequenced on an Illumina MiSeq instrument using 300/200 base pair (bp) paired-end sequencing. Approximately 18.3 million sequencing reads were analyzed using a modified version of SURPI (Sequence-Based Ultra-Rapid Pathogen Identification)[11], a computational pipeline for detection of microbes, including viruses, from next-generation sequencing data. Briefly, after detection of viral sequences aligning to human endogenous retroviruses (HERVs) with an initial run using SURPI, the pipeline was rerun with the following modifications: (1) raw sequencing reads were preprocessed by adapter trimming and low-quality / low-complexity filtering (generating ~1.3 to 3.5 million reads per sample), (2) the human computational subtraction step was skipped to retain human endogenous viral sequences, and (3) preprocessed reads were aligned to the viral portion of the NCBI (National Center for Biotechnology Information) NT database to detect HERV sequences. Viral reads were identified as HERVs using a stringent edit distance requirement of 0 (no mismatches) across 75 bp of sequence. HERV reads were also taxonomically classified to the appropriate rank (family, genus, species, or subspecies/strain) by use of an in-house developed classification algorithm using the SNAP nucleotide aligner (v0.15)[11]. Heat maps were generated using matrix2png[12].

CyTOF (single cell mass cytometry)

Details of the CyTOF method were described previously[13]. In brief, PBMC were stained with metal-conjugated antibodies (listed below) and analyzed with a mass cytometer. A subset of the antibodies was obtained pre-labeled by Fluidigm (San Francisco, CA) and others were conjugated with metals in-house, using MaxPAR antibody conjugation kit (Fluidigm, San Francisco, CA). $1X10^6$ cells were used for each sample. After staining with cisplatin for viability evaluation[14], cells were treated with 002% Saponin (Sigma, St. Louis, MO) in cell staining media (CSM, low barium PBS with 0.5% BSA, 0.02% NaN3), then stained with barcoding dye for 15 min for identification, to enable pooling for processing and measurement as a single multiplexed sample[13]. Cells were stained with surface markers for one hr at room temperature. After permeabilization with methanol for 10 min at 4^oC, cells were stained with intracellular markers for one hr at room temperature, then with DNA intercalator (Fluidigm, South San Francisco, CA) overnight at 4^oC. Cells were washed with CSM twice between individual steps and washed three times with MilliQ water before the samples were analyzed with mass cytometer (CyTOF2, Fluidigm, South San Francisco, CA). Stained cells were analyzed on mass cytometer at event rate of 400-500 cells per second. Data files were concatenated. The data were normalized using NormalizerR2013b and de-barcoded using the Matlab DebarcoderR2013b. Gating was performed in http://nolanlab.cytobank.org[15]. The data were transformed to arcsinh values by taking the inverse hyperbolic sine of the raw data. The arcsinh ratio is the difference between the median arcsinh values of the two samples. For Figure 2D, all the data from PAH and controls are shown as arcsinh ratio

over assay control. For Figure 4F, the data shows HERV-K dUTPase-treated over untreated (control) PBMCs (Stanford Blood Bank).

CyTOF antibodies:

(i) PAH vs. control samples

Isotope	Antigen	Clone	Supplier
Y 89	CD45	HI30	Fluidigm, South San Francisco, CA
Er 170	CD3	UCHT1	Fluidigm, South San Francisco, CA
Nd 142	CD19	HIB19	Fluidigm, South San Francisco, CA
Yb 176	CD7	M-T701	BD Biosciences, San Jose, CA
Nd 143	CD11c	Bu15	Biolegend, San Diego, CA
Gd 160	CD14	M5E2	Biolegend, San Diego, CA
Bi 209	CD16	3G8	Fluidigm, South San Francisco, CA
In 115	HLADR	L243	Trace Sciences, Richmond Hill, Canada
Pr 141	cPARP	F21-852	BD Biosciences, San Jose, CA

(ii) HERV-K dUTPase treatment of PBMC

Isotope	Antigen	Clone	Phosphorylation site	Supplier
In 115	CD45	HI30	N/A	Biolegend, San Diego, CA
Er 170	CD3	UCHT1	N/A	Fluidigm, South San Francisco, CA
Nd 142	CD19	HIB19	N/A	Fluidigm, South San Francisco, CA
Yb 174	HLADR	L243	N/A	Fluidigm, South San Francisco, CA
Dy 162	CD69	FN50	N/A	Fluidigm, South San Francisco, CA
Pr 141	Caspase3	C92-605	N/A	BD Biosciences, San Jose, CA

Isotope	Antigen	Clone	Phosphorylation site	Supplier
Eu 153	pSTAT1	58D6	pY701	Fluidigm, South San Francisco, CA
Gd 156	pSTAT3	4	pY705	BD Biosciences, San Jose, CA
Dy 164	pSTAT5	47	pY694	BD Biosciences, San Jose, CA
Gd 158	pMAPKAPK2	27B7	pT334	Cell Signaling Technology, Danvers, MA
Sm 149	pNFkB	K10-895.12.50	pS529	BD Biosciences, San Jose, CA
Sm 152	pAKT	D9E	pS473	Fluidigm, South San Francisco, CA
Er 167	pERK	D13.14.4E	pT202/Y204	Fluidigm, South San Francisco, CA

N/A, not applicable

Rat model for the induction of pulmonary hypertension by HERV-K dUTPase

The experimental protocol used in this study was approved by the Animal Care Committee at Stanford University following the published guidelines of the National Institutes of Health and the American Physiological Society. Adult male Sprague-Dawley rats (7 wks, 180-200 g) were randomly assigned to a control or treatment group. Rats were either untreated or given a single subcutaneous dose of SU5416 (20 mg/kg body weight) one day prior to the first of three weekly intravenous injections of HERV-K dUTPase (0.2 mg/kg body weight). Rats in the control group were treated with saline vehicle. Twenty-one days after the first HERV-K dUTPase injection, cardiac function, right ventricular systolic pressure and right ventricular hypertrophy were assessed as previously described[1]. In brief, cardiac function was measured by Vivid 7 ultrasound machine (GE Healthcare, Pittsburgh, PA) and 13-MHz linear array transducer. RVSP

was measured by inserting 1.4F Millar catheter (Millar Instruments, Houston, TX) via right jugular vein. Pressure measurements were repeated three times. Data were collected by Power Lab Data Acquisition system (AD Instruments, Colorado Springs, CO) and analyzed by LabChart software (AD Instruments, Colorado Springs, CO). Right ventricular hypertrophy was assessed by the weight ratio of the RV to LV plus septum. Isoflurane anesthesia (1.5%, 1 liter/min oxygen) was used during these procedures. After hemodynamic measurements, the lungs were flushed with saline. Right lungs were snap-frozen in liquid nitrogen and stored at -80^{o}C for ELISA. Left lungs were fixed with 10% formalin for histology. For histology, staining methods are described above. Images were acquired using Leica DMLB microscope (Leica, Buffalo Grove, IL). Quantification of muscularization and arterial number relative to alveoli was conducted in a blinded manner as described below. For IL6 measurement by ELISA, 20 μg of tissues was homogenized per the manufacturer's protocol. After centrifugation, total protein concentration of supernatant was measured and prepared in PBS at 0.5 μg/μL total protein.

Quantification of Immunohistochemistry

Evaluation of muscularized arteries: To evaluate the distal pulmonary arteries (DPAs) at alveolar duct and alveolar wall level, we counted DPAs in six randomly chosen low magnification (200X) fields per rat, in the SMA and vWF double stained immunofluorescent images. The artery was defined as muscularized if a thick double line of SMA staining was observed in multiple areas. The ratio of muscularized DPAs over total DPAs was calculated.

Loss of distal vessels: We counted DPAs as described above and alveoli in six randomly chosen low magnification (200X) fields per rat in Movat stained sections, and calculated the ratio of total counted DPAs over total alveoli.

Statistical Analysis

Data were analyzed using Prism 6.0 (GraphPad Software, La Jolla, CA). Statistical significance was determined by one-way ANOVA followed by Dunnett's test or Tukey's test of multiple comparisons when more than two groups were being compared. When only two groups were compared, we used Student's t-test. For some experiments, as indicated in the figure legends, we applied the Welch or Mann Whitney test depending on the data distribution, i.e., when the distribution was not normal we used the Mann-Whitney and when the variance was unequal by F-test, we used the Welch. A P-value of <0.05 was considered significant. Data are shown as mean $\pm$ SEM or median with interquartile range depending on the test applied. For target identification of immune complexes by mass spectrometry, significance analysis of microarray (SAM) was applied with false discovery rate (FDR) cutoff of 5% [9]. For signaling data by CyTOF, Bonferroni-adjusted P-value ($P=7.14X10^{-3}$) was applied to signaling response with arcsinh ratio $>|0.2|$[13].

Accession Numbers

Next-generation sequencing data with human sequences removed, using BLASTn to the human genome at a low-stringency cutoff of 10^{-5} have been publicly deposited in the NIH Sequence Read Archive (SRA accession number SRP056561).

Supplemental Tables:

Supplemental Table 1: Characteristics of PAH patients

Patient	PAH Diagnosis[a]	Age - Gender	Race	PAP[b] mean (mmHg)	PVR[c] (Wood Units)	6 Min[d] Walk (m)	PAH Medications[e]	Study
PAH-01	HPAH (BMPR2 mutation)	33-F	AA	48	15.57	326	epoprostenol, bosentan, sildenafil, treprostinil	tLTs, IHC, qPCR (lung, PAEC, iPSC, iPSC-EC)
PAH-02	HPAH	47-M	White	62	11.95	282	bosentan, sildenafil, epoprostenol	SAMHD1 IC
PAH-03	IPAH	39-F	Asian	47	N/A	161	epoprostenol, bosentan, ambrisentan, sildenafil	SAMHD1 IC, WB, viral screen
PAH-04	IPAH	58-F	White	50	N/A	206	bosentan, tresprostinil, sildenafil, epoprostenol	tLT, SAMHD1 IC
PAH-05	IPAH	28-F	White	37	6.38	434	sildenafil, epoprostenol, bosentan	tLT, SAMHD1 IC
PAH-06	IPAH	27-F	AA	55	N/A	316	sildenafil, treprostinil (inhaled)	tLT, SAMHD1 IC
PAH-07	IPAH	16-F	White	80	N/A	348	bosentan, ambrisentan, epoprostenol, sildenafil, tresprostinil	tLT
PAH-08	IPAH	41-F	Unknown	43	N/A	335	tresprostinil, bosentan, sildenafil	tLT
PAH-09	IPAH	40-F	White	47	N/A	294	ambrisentan, sildenafil, iloprost, epoprostenol	tLT
PAH-10	IPAH	29-F	AA	41	N/A	339	epoprostenol, ambrisentan, sildenafil	SAMHD1 IC
PAH-11	IPAH	24-M	Asian	48	9.56	356	sildenafil, ambrisentan, epoprostenol, bosentan	SAMHD1 IC
PAH-12	HPAH	56-F	White	75	N/A	372	epoprostenol, bosentan, ambrisentan, sildenafil	SAMHD1 IC, MS

Patient	PAH Diagnosis[a]	Age - Gender	Race	PAP[b] mean (mmHg)	PVR[c] (Wood Units)	6 Min[d] Walk (m)	PAH Medications[e]	Study
PAH-13	IPAH	49-F	White	75	16.76	326	ambrisentan, sildenafil, epoprostenol	tLT, SAMHD1 IC, MS, WB, IHC, viral screen, qPCR (lung)
PAH-14	HPAH (BMPR2 mutation)	27-F	White	69	12.11	360	sildenafil, tresprostinil bosentan iloprost	qPCR (lung, PAEC, PASMC)
PAH-15	IPAH	45-M	White	48	11.08	293	treprostinil bosentan sildenafil epoprostenol	SAMHD1 IC.
PAH-16	HPAH (BMPR2 mutation)	33-F	White	48	9.74	288	bosentan treprostinil sildenafil epoprostenol	SAMHD1 ICs, qPCR (lung, PASMC)
PAH-17	IPAH	15-F	White	102	25.24	387	sildenafil epoprostenol	tLT, qPCR (lung)
PAH-18	HPAH (SMAD9 mutation) +APAH (CHD)	16-F	Asian	92	16.15	512	sildenafil treprostinil bosentan epoprostenol	tLT, SAMHD1 IC, WB, IHC, viral screen, qPCR (lung)
PAH-19	IPAH	25-F	Asian	87	20.96	201	epoprostenol sildenafil bosentan	tLTs, qPCR (lung)
PAH-20	IPAH	55-F	AA	53	12.29	273	sildenafil bosentan epoprostenol	tLTs, SAMHD1 IC, MS, IHC, qPCR (lung)
PAH-21	IPAH	25-M	White	36	N/A	511	epoprostenol sildenafil treprostinil	SAMHD1 IC, WB, qPCR
PAH-22	IPAH	56-F	White	57	11.41	137	sildenafil ambrisentan treprostinil	SAMHD1 IC, qPCR (PAEC, iPSC, iPSC-EC)
PAH-23	IPAH	41-F	White	55	9.84	472	sildenafil bosentan epoprostenol	tLTs, SAMHD1 IC, WB, viral screen, qPCR (lung, PAEC)
PAH-24	IPAH	58-F	White	47	12.66	642	bosentan sildenafil	CyTOF
PAH-25	IPAH	27-F	White	27	5.26	707	tadalafil	CyTOF
PAH-26	IPAH	47-F	AA	47	5.5	344	treprostinil (inhaled) tadalafil	CyTOF

Patient	PAH Diagnosis[a]	Age - Gender	Race	PAP[b] mean (mmHg)	PVR[c] (Wood Units)	6 Min[d] Walk (m)	PAH Medications[e]	Study
PAH-27	IPAH	36-M	Asian	70	12.7	488	treprostinil (inhaled) ambrisentan sildenafil	CyTOF
PAH-28	IPAH	27-F	White	40	7.82	548	treprostinil (inhaled) sildenafil	CyTOF
PAH-29	IPAH	36-M	Other	44	7.17	481	tadalafil	CyTOF
PAH-30	IPAH	29-F	White	53	8.95	590	treprostinil (subcutaneous) tadalafil	CyTOF
PAH-31	IPAH	50-F	White	40	5.99	550	ambrisentan sildenafil	CyTOF
PAH-32	IPAH	46-F	AA	52	10.25	572	None	CyTOF
PAH-33	IPAH	36-F	Asian	33	3.83	594	treprostinil (inhaled) tadalafil	CyTOF
PAH-34	IPAH	46-F	Asian	57	13.69	518	epoprostenol sildenafil	qPCR (monocytes)
PAH-35	IPAH	35-F	White	61	26.96	366	None	qPCR (monocytes)
PAH-36	IPAH	53-F	White	50	12.6	238	None	qPCR (monocytes)
PAH-37	IPAH	20-F	White	33	6.84	675	ambrisentan tadalafil	qPCR (monocytes)
PAH-38	IPAH	46-F	White	58	11.11	232	treprostinil (inhaled) sildenafil	qPCR (monocytes)
PAH-39	IPAH	40-M	White	64	73	420	sildenafil, ambrisentan, treprostinil	qPCR (PAEC, iPSC, iPSC-EC)
PAH-40	IPAH	11-F	White	95	N/A	244	sildenafil, ambrisentan, epoprostenol, treprostinil	qPCR (PASMC)
PAH-41	IPAH	39-F	Unknown	69	14.97	262	sildenafil, bosentan iloprost, epoprostenol	qPCR (PAEC, iPSC, iPSC-EC)
PAH-42	HPAH	37-M	White	77	14.22	309	sildenafil, sitaxsentan, ambrisentan, epoprostenol, Imatinib(investigational medication), treprostinil	qPCR (PASMC)
PAH-43	HPAH (BMPR2 Mutation)	N/A -M	White	N/A	N/A	N/A	N/A	qPCR (iPSC)

Patient	PAH Diagnosis[a]	Age - Gender	Race	PAP[b] mean (mmHg)	PVR[c] (Wood Units)	6 Min[d] Walk (m)	PAH Medications[e]	Study
PAH-44	HPAH (BMPR2 Mutation)	N/A -F	White	N/A	N/A	N/A	N/A	qPCR (iPSC)
PAH-45	HPAH (BMPR2 Mutation)	N/A -F	White	N/A	N/A	N/A	N/A	qPCR (iPSC)

[a] Diagnosis: Pulmonary arterial hypertension (PAH) classification: IPAH, Idiopathic PAH; HPAH, hereditary PAH, known mutation as stated; APAH, Associated PAH; CHD, congenital heart disease

[b] PAP, Mean pulmonary arterial pressure. Data were obtained from catheterization study performed closest to transplantation or blood draw.

[c] PVR, Pulmonary vascular resistance. Data were obtained from catheterization study performed closest to transplantation or blood draw.

[d] 6 Min Walk = distance walked in six minutes. Data were obtained from study performed closest to transplantation or blood draw.

[e] PAH medications: For samples provided by the PAH biobank (CyTOF experiments) we list current medications at the time of blood draw. All others, medications are listed according to total drug exposure during treatment period up to transplantation, not necessarily in combination.

AA, African American

IHC, immunohistochemistry of SAMHD1

MS, complement 1q (C1q) mass spectroscopy

NA, data not available

qPCR (lung), evaluation of HERV-K(II) envelope and HERV-K dUTPase in the lung, by qPCR

qPCR (monocytes, PAEC, PASMC, iPSC, iPSC-EC), evaluation of HERV-K dUTPase in this cell type, by qPCR

SAMHD1 ICs, immunohistochemistry of SAMHD1 in ICs

tLTs, immunohistochemistry to detect tertiary lymphoid tissues

Viral screen, screen for HERV-K viruses

WB, expression of SAMHD1 assayed by western immunoblot

CyTOF, single cell mass cytometry

Supplemental Table 2: Characteristics of Controls (unused donor lungs or healthy volunteers)

For definitions, see Supplemental Table 1.

Patient	Age - Gender	Race	Cause of Death	Study
CON-01	18-M	White	Gunshot wound to the head	SAMHD1 IC
CON-02	26-M	White	Cerebrovascular accident/Stroke	tLT, SAMHD1 IC
CON-03	14-M	White	Gun shot wound to head	tLT
CON-04	55-M	White	Anoxia/cardiovascular/ natural causes	SAMHD1 IC, WB
CON-05	14-M	White	Cardiac arrest secondary to diabetic ketoacidosis	tLT
CON-06	54-F	White	Cerebrovascular accident /stroke	qPCR (lung)
CON-07	28-F	White	Anoxia following motor vehicle accident	tLT, SAMHD1 IC, WB, IHC, viral screen, qPCR (lung)
CON-08	62-M	White	Cerebrovascular/ intercranial hemorrhage/stroke	SAMHD1 IC
CON-09	47-M	White	Motor vehicle accident	qPCR (lung, PAEC, iPSC-EC, iPSC)
CON-10	56-F	White	Cerebrovascular accident	tLT, IHC, qPCR (lung)
CON-11	49-F	White	Intracranial hemorrhage	qPCR
CON-12	30-M	White	Head trauma due to motor vehicle accident	tLT, IHC, qPCR (lung)
CON-13	55-F	Unknown	Intracranial stroke/hemorrhage	tLT, qPCR (lung, PAEC)
CON-14	12-M	AA	Brain death/cerebral edema/diabetic ketoacidosis/diabetes-type1	tLT
CON-15	40-F	White	Extensive intracranial injury/subarachnoid hemorrhage secondary to motor vehicle accident	Viral screen
CON-16	45-F	White	Cerebrovascular accident/ subarachnoid hemorrhage	SAMHD1 IC
CON-17	25-M	White	Cerebrovascular/ intracranial hemorrhage/stroke	tLT, IHC, qPCR (lung)

Patient	Age - Gender	Race	Cause of Death	Study
CON-18	60-M	White	Type A aortic dissection with brain death	SAMHD1 IC, WB
CON-19	54-M	White	Choking with anoxic brain injury	SAMHD1 IC
CON-20	41-F	White	Grade 4 subarachnoid hemorrhage, ruptured anterior cerebral artery aneurysm	tLT, SAMHD1 IC, MS, WB, viral screen, qPCR (lung)
CON-21	17-M	White	Head injury progression to brain death secondary to motor vehicle accident	tLT
CON-22	49-M	White	Intracranial hemorrhage	SAMHD1 IC, MS, WB
CON-23	43-M	White	Fatal gun shot to head	tLT, SAMHD1 IC
CON-24	19-M	White	Anoxic brain injury	tLT, MS, viral screen, qPCR (lung)
CON-25	19-M	AA	Anoxia of brain	tLT, SAMHD1 IC
CON-26	52-F	White	Hypoxic brain death	tLT
CON-27	59-F	White	N/A – Healthy volunteer	CyTOF
CON-28	27-F	White	N/A – Healthy volunteer	CyTOF
CON-29	47-F	White	N/A – Healthy volunteer	CyTOF
CON-30	36-M	Asian	N/A – Healthy volunteer	CyTOF
CON-31	28-F	White	N/A – Healthy volunteer	CyTOF
CON-32	36-M	White	N/A – Healthy volunteer	CyTOF
CON-33	46-F	White	N/A – Healthy volunteer	CyTOF
CON-34	51-F	AA & White	N/A – Healthy volunteer	CyTOF
CON-35	30-F	White	N/A – Healthy volunteer	qPCR (monocytes)
CON-36	35-F	Asian	N/A – Healthy volunteer	qPCR (monocytes)
CON-37	52-F	White	N/A – Healthy volunteer	qPCR (monocytes)

Patient	Age - Gender	Race	Cause of Death	Study
CON-38	46-F	White	N/A – Healthy volunteer	qPCR (monocytes)
CON-39	57M	White	N/A – Healthy volunteer	qPCR (monocytes)
CON-40	45-M	White	Anoxia	qPCR (PAEC, iPSC-EC, iPSC)
CON-41	43-F	White	Cerebrovascular/Stroke	qPCR (PAEC, iPSC-EC, iPSC, PASMC)
CON-42	33-F	White	Head trauma. Blunt injury	qPCR (PAEC, iPSC-EC, iPSC)
CON-43	1-M	White	Anoxia/Drowning	MTT (PASMC)
CON-44	46-M	Asian	Cerebrovascular/Stroke	qPCR (PASMC)
CON-45	36-F	White	Subarachnoid hemorrhage	qPCR (PASMC)
CON-46	51-M	White	Cerebrovascular accident	qPCR (PAEC)
CON-47	N/A - M	White	N/A	qPCR (iPSC)
CON-48	N/A – F	White	N/A	qPCR (iPSC)
CON-49	N/A - F	White	N/A	qPCR (iPSC)

Supplemental Figures and Legends:

Supplemental Figure 1: Gating strategy for classical dendritic cells (cDC) or B-cells of PAH patients and controls, used in the experiments shown in Figures 2D, 4E and 4F.

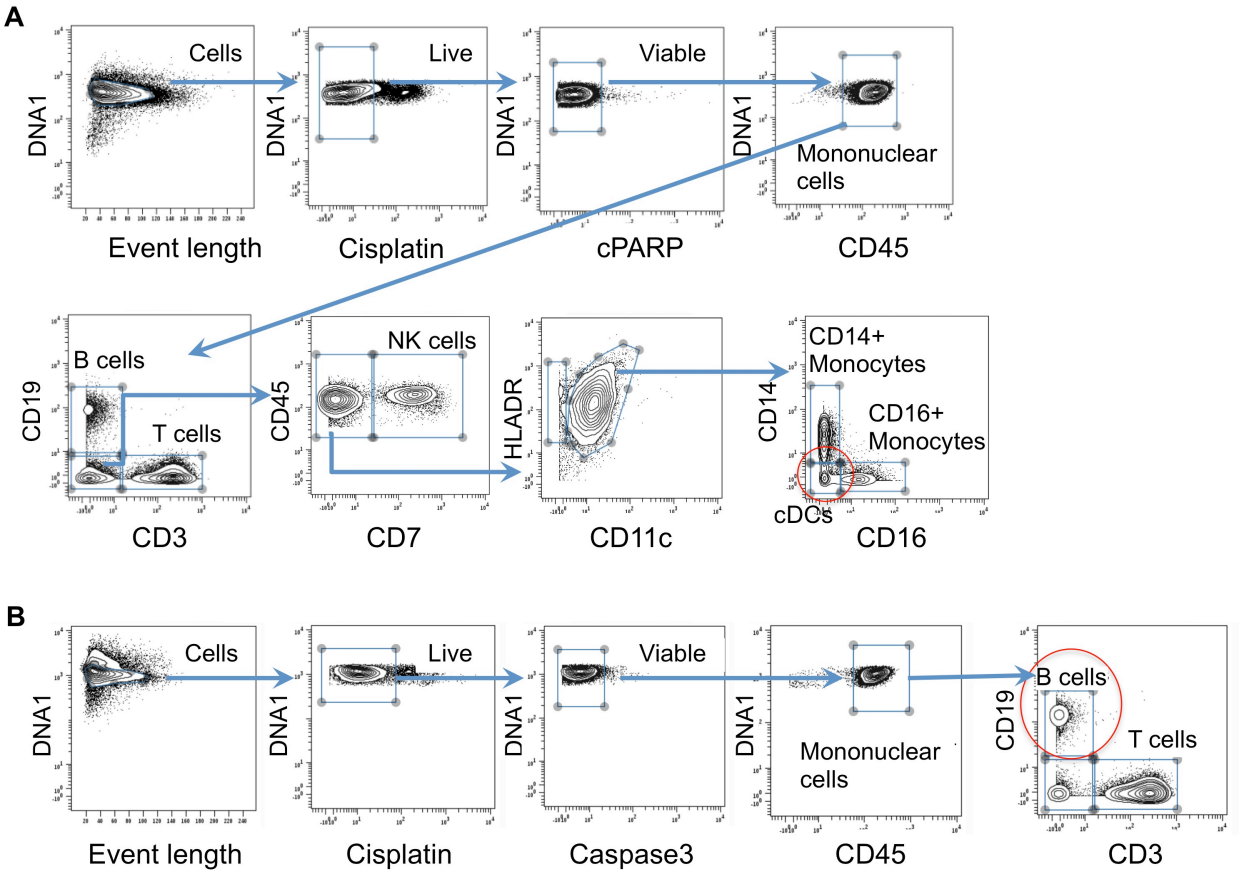

A schematic representation of the gating strategies used to define viable cells and immune cells types. **(A)** Gating for classical dendritic cells (cDC), used in rhe experiment shown in Figure 2D. **(B)** Gating for B-cells, used in the experiments shown in Figure 4E, F. Data are from representative samples. Gates and plots were created using cytobank.org. Live cells were gated by Cisplatin then viable cells were further gated by cPARP (A) or by Caspase 3 (B). NK cells: natural killer cells, cDC: classical dendritic cells, cPARP: cleaved PARP.

Supplemental Figure 2: HERV-K dUTPase and apoptosis in pulmonary arterial endothelial cell (PAEC) and monocyte co-cultures, IL6 antibody efficacy, HERV-K dUTPase and PASMC proliferation, lipopolysaccharide (LPS) and HERV-K dUTPase mRNA in PAEC, and in PAH vs. control iPSC-EC, PAEC and PASMC.

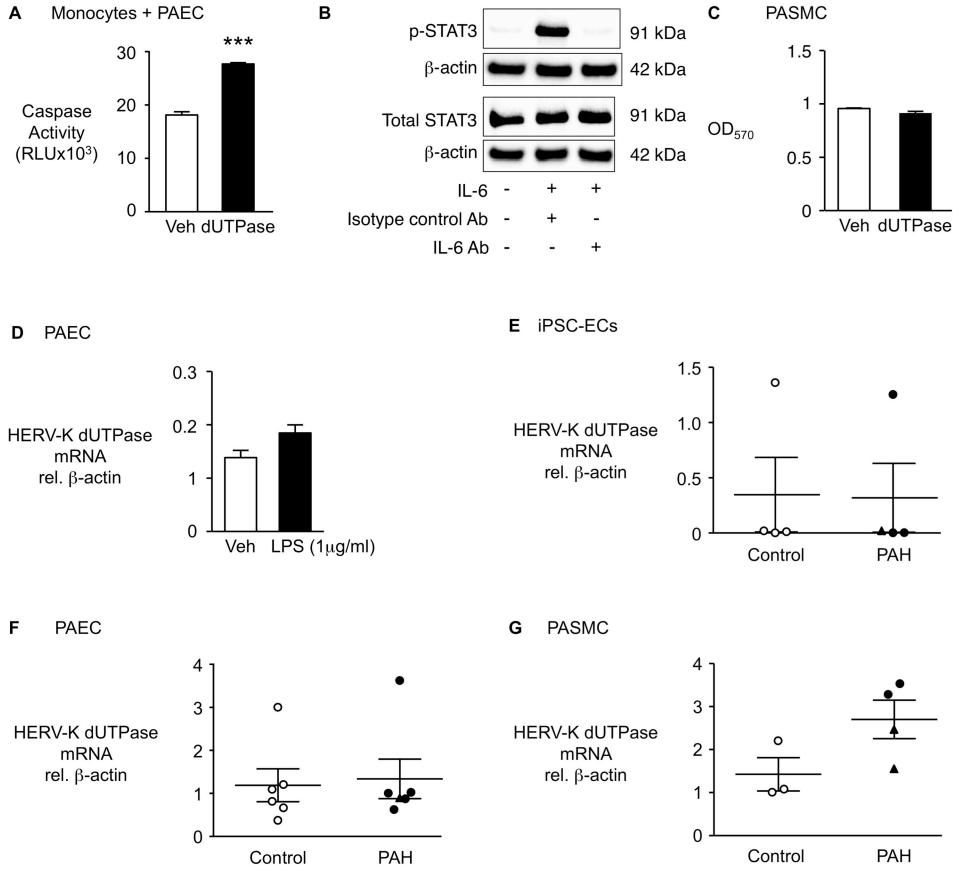

(A) Monocytes were treated with 10 μg/mL HERV-K dUTPase on a cell culture insert and then co-cultured with PAEC subjected to serum withdrawal media overnight (0% FBS). Apoptosis was assessed by Caspase-Glo 3/7 assay (n=3). **(B)** Corresponding to Figure 5B, the efficiency of neutralizing IL6 antibody was confirmed by blocking pSTAT3, assessed by immunoblot. **(C)** PASMC were treated with 10 μg/mL HERV-K dUTPase and proliferation was assessed by MTT assay (n=4) at 48 hr. **(D)** HERV-K dUTPase mRNA by qPCR in 1 μg/mL LPS-treated PAEC (n=3). **(E)** HERV-K dUTPase mRNA by qPCR in iPSC-EC from PAH patients (n=4) and controls (n=4). **(F)** HERV-K dUTPase mRNA by qPCR in PAEC from PAH patients (n=6) and controls (n=6). **(G)** HERV-K dUTPase mRNA by qPCR in PASMC from PAH patients (n=4) and controls (n=3). Ranges represent mean ± SEM (A, C-G). ***P<0.001 by Student's t-test. Closed symbols (PAH), open symbols (Controls), closed triangles hereditary PAH (HPAH).

Supplemental Figure 3: HERV-K dUTPase does not affect left ventricular function or the number of pulmonary vessels in a rat model of pulmonary hypertension.

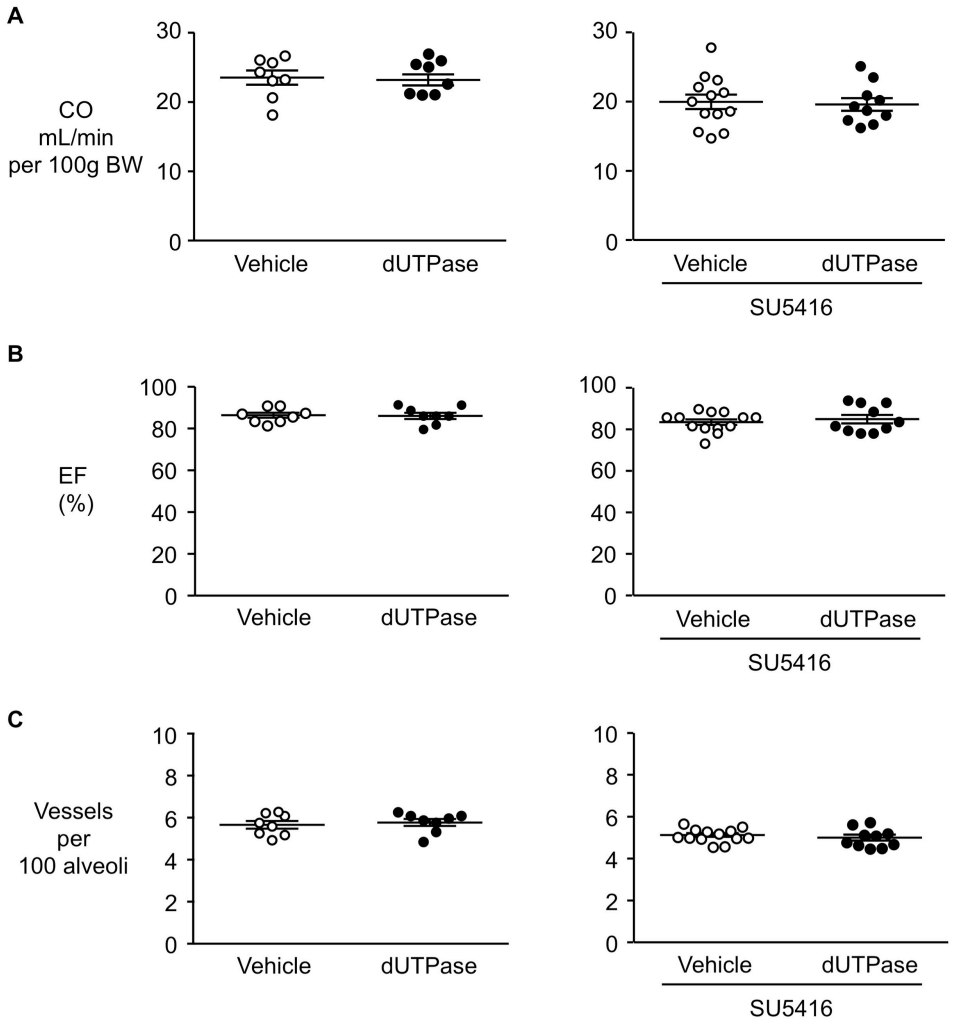

Rats were pre-treated with or without the VEGF receptor blocker SU5416 then subsequently given three weekly injections of HERV-K dUTPase or vehicle (saline). Saline (n=8), HERV-K dUTPase (n=8), SU5416+Saline (n=13) or SU5416+HERV-K dUTPase (n=10) as described for Figure 6. **(A)** Cardiac output (CO) and **(B)** ejection fraction (EF) were evaluated by echocardiogram. **(C)** Vessels and alveoli were counted in Movat-stained lung sections from the rats. Ranges represent mean ± SEM. We found no significant difference between the groups by Student's t-test.

Supplemental Material References

1. Sawada H, Saito T, Nickel NP, Alastalo TP, Glotzbach JP, Chan R, Haghighat L, Fuchs G, Januszyk M, Cao A, Lai YJ, Perez Vde J, Kim YM, Wang L, Chen PI, Spiekerkoetter E, Mitani Y, Gurtner GC, Sarnow P, Rabinovitch M. Reduced BMPR2 expression induces GM-CSF translation and macrophage recruitment in humans and mice to exacerbate pulmonary hypertension. *J Exp Med*. 2014;211:263-280.
2. Sa S, Gu M, Chappell J, Shao NY, Ameen M, Elliott KA, Li D, Grubert F, Li CG, Taylor S, Cao A, Ma Y, Fong R, Nguyen L, Wu JC, Snyder MP, Rabinovitch M. Induced pluripotent stem cell model of pulmonary arterial hypertension reveals novel gene expression and patient specificity. *Am J Respir Crit Care Med*. 2017;195:930-941.
3. Tojais NF, Cao A, Lai YJ, Wang L, Chen PI, Alcazar MAA, de Jesus Perez VA, Hopper RK, Rhodes CJ, Bill MA, Sakai LY, Rabinovitch M. Codependence of bone morphogenetic protein receptor 2 and transforming growth factor-beta in elastic fiber assembly and its perturbation in pulmonary arterial hypertension. *Arterioscler Thromb Vasc Biol*. 2017;37:1559-1569.
4. Gu M, Shao NY, Sa S, Li D, Termglinchan V, Ameen M, Karakikes I, Sosa G, Grubert F, Lee J, Cao A, Taylor S, Ma Y, Zhao Z, Chappell J, Hamid R, Austin ED, Gold JD, Wu JC, Snyder MP, Rabinovitch M. Patient-specific ipsc-derived endothelial cells uncover pathways that protect against pulmonary hypertension in BMPR2 mutation carriers. *Cell Stem Cell*. 2017;20:490-504 e495.

5. Ariza ME, Williams MV. A human endogenous retrovirus k dutpase triggers a th1, th17 cytokine response: Does it have a role in psoriasis? *J Invest Dermatol*. 2011;131:2419-2427.

6. Lawrie A, Spiekerkoetter E, Martinez EC, Ambartsumian N, Sheward WJ, Maclean MR, Harmar AJ, Schmidt AM, Lukanidin E, Rabinovitch M. Interdependent serotonin transporter and receptor pathways regulate s100a4/mts1, a gene associated with pulmonary vascular disease. *Circ Res*. 2005;97:227-235.

7. Tuominen VJ, Ruotoistenmaki S, Viitanen A, Jumppanen M, Isola J. Immunoratio: A publicly available web application for quantitative image analysis of estrogen receptor (er), progesterone receptor (pr), and ki-67. *Breast Cancer Res*. 2010;12:R56.

8. Wisniewski JR, Zougman A, Nagaraj N, Mann M. Universal sample preparation method for proteome analysis. *Nat Methods*. 2009;6:359-362.

9. Roxas BA, Li Q. Significance analysis of microarray for relative quantitation of lc/ms data in proteomics. *BMC Bioinformatics*. 2008;9:187.

10. Greninger AL, Chen EC, Sittler T, Scheinerman A, Roubinian N, Yu G, Kim E, Pillai DR, Guyard C, Mazzulli T, Isa P, Arias CF, Hackett J, Schochetman G, Miller S, Tang P, Chiu CY. A metagenomic analysis of pandemic influenza a (2009 h1n1) infection in patients from north america. *PLoS One*. 2010;5:e13381.

11. Naccache SN, Federman S, Veeraraghavan N, Zaharia M, Lee D, Samayoa E, Bouquet J, Greninger AL, Luk KC, Enge B, Wadford DA, Messenger SL, Genrich GL, Pellegrino K, Grard G, Leroy E, Schneider BS, Fair JN, Martinez MA, Isa P,

Crump JA, DeRisi JL, Sittler T, Hackett J, Jr., Miller S, Chiu CY. A cloud-compatible bioinformatics pipeline for ultrarapid pathogen identification from next-generation sequencing of clinical samples. *Genome Res*. 2014;24:1180-1192.

12. Pavlidis P, Noble WS. Matrix2png: A utility for visualizing matrix data. *Bioinformatics*. 2003;19:295-296.
13. Gaudilliere B, Fragiadakis GK, Bruggner RV, Nicolau M, Finck R, Tingle M, Silva J, Ganio EA, Yeh CG, Maloney WJ, Huddleston JI, Goodman SB, Davis MM, Bendall SC, Fantl WJ, Angst MS, Nolan GP. Clinical recovery from surgery correlates with single-cell immune signatures. *Sci Transl Med*. 2014;6:255ra131.
14. Fienberg HG, Simonds EF, Fantl WJ, Nolan GP, Bodenmiller B. A platinum-based covalent viability reagent for single-cell mass cytometry. *Cytometry A*. 2012;81:467-475.
15. Bendall SC, Simonds EF, Qiu P, Amir el AD, Krutzik PO, Finck R, Bruggner RV, Melamed R, Trejo A, Ornatsky OI, Balderas RS, Plevritis SK, Sachs K, Pe'er D, Tanner SD, Nolan GP. Single-cell mass cytometry of differential immune and drug responses across a human hematopoietic continuum. *Science*. 2011;332:687-696.